Supply-demand analysis of anaerobic free-energy metabolism in *Zymomonas mobilis*

Christiaan Crous

Thesis presented in partial fulfilment of the requirements for the degree of Master of Science at Stellenbosch University.

Department of Biochemistry
University of Stellenbosch
Private Bag X1, 7602 Matieland, South Africa

Supervisor: Prof JM Rohwer
Co-supervisor: Prof JL Snoep

December 2011

Declaration

By submitting this dissertation electronically, I declare that the entirety of the work contained therein is my own, original work, that I am the owner of the copyright thereof (unless to the extent explicitly otherwise stated) and that I have not previously in its entirety or in part submitted it for obtaining any qualification.

Date: 3 October 2011

Opsomming

Fermentasie in *Zymomonas mobilis* word beskryf as ‘n kataboliese snelweg, waar glikolitiese en fermentatiewe ensieme 50% van totale oplosbare proteïene in die sel uitmaak. Hoewel dié fermentasie een van die vinnigstes is wat tot op hede waargeneem is, is die omskakeling van glukose na etanol een van die mees ondoeltreffende energie-ekstraksies in die natuur. Dié lae energie-opbrengs, soos waarneembaar in fermentasie in *Zymomonas mobilis,* kan toegeskryf word aan die Entner-Doudoroff metaboliese pad. Hierdie metaboliese pad lewer slegs die helfte van die energie-opbrengs per mol substraat vergeleke met die meer bekende Embden-Meyerhof-Parnas glikolitiese pad.

Die navorsing in hierdie tesis is deel van ‘n omvattende projek wat poog om die regulering van glikolise in verskillende mikro-organismes (*Z. mobilis*, *Escherichia coli*, *Saccharomyces cerevisiae* en *Lactococcus lactis*) te vergelyk. Dié organismes is gekies op grond van die uiteenlopende glikolitiese meganismes waarvan hulle gebruik maak. Ten einde die reguleringsgedrag van meganisties verskillende vry-energie produksieweë m.b.v. vraag-aanbod analise te vergelyk, moet glikolitiese regulering eers onder eenderse eksperimentele kondisies (b.v. nie-groeiende selkulture) gekwantifiseer kan word.

Die hoofdoel van hierdie tesis was om die belang van anaerobiese vry-energie produksie vir die regulering van die Entner-Doudoroff glikolitiese pad in *Z. mobilis* te kwantifiseer. Hiervoor is van Metaboliese kontrole-analise (MKA) en vraag-aanbodanalise (‘n uitbreiding van MKA) gebruik gemaak. MKA is ‘n tegniek waarmee die effek wat ‘n metaboliese parameter (soos metaboliese deel-konservering) op ‘n spesifieke bestendige toestand-veranderlike (soos fermentasiefluksie) het, gekwantifiseer kan word. Vraag-aanbodanalise daarenteen, bied ‘n kwantitatiewe raamwerk waardeur die regulatoriese belang van sellulêre kommoditeite (byvoorbeeld anaerobiese vry-energie) geanaliseer kan word. Tydens laasgenoemde proses word die elastisiteit van die anaerobiese vry-energie aanbod en die elastisiteit van die vraag vergelyk. Op hierdie manier kan die mate van beheer wat die onderskeie reaksieblokkie oor die fluksie deur anaerobiese vry-energie metaboliese paaie, sowel as oor die sellulêre vry-energie toestand (ATP/ADP verhouding), bepaal word.

In hierdie werk is die regulering van anaerobiese vry-energie metabolisme in *Z. mobilis* ondersoek deur van ‘n eksperimentele benadering gebruik te maak. Die sleuteleienskappe van dié benadering was om kernmagnetiese-resonansiespektroskopie (KMR spektroskopie) te gebruik om metabolietkonsentrasies te meet, en om van nie-groeiende kondisies gebruik te maak vir die vraag-aanbod eksperimente. Metabolietkonsenstrasies kon aaneenlopend bepaal word sonder die gebruik van monsternemingstegnieke wat die reaksie sou kon beïnvloed. Eksterne invloede op die fermentasiegedrag kon ook uitgesluit word deur van nie-groeiende kondisies gebruik te maak, sodat die waargenome fermentasiegedrag uitsluitelik aan die anaerobiese vry-energie toestand toegeskryf kan word.

Glukose fermentasie was ondersoek in wilde tipe *Z. mobilis*, en in drie rekombinante wat onderskeidelik ‘n glukose fasiliteerder ooruitdrukkingsplasmied (TCDB 2.A.1.1.4), ‘n glukose-6-fosfaat dehidrogenase ooruitdrukkingsplasmied (EC 1.1.1.49), en ‘n nie-uitdrukkingsplasmied bevat het. Die ATP vraag in die wilde tipe en die nie-uitdrukkingsrekombinant is geperturbeer deur titrasies met asynsuur as ontkoppelaar. Die resultate toon dan die anaerobiese vry-energievraag, sowel as die glukose fasiliteerder en glukose-6-fosfaat dehidrogenase, die fluksie van etanolproduksie in *Z. mobilis* beheer. Die Entner-Doudoroff glikolitiese produksie-aktiwiteit was sensitief vir veranderinge in die ATP/ADP verhouding (elastisiteite was tussen -0.31 en -0.49) en die NTP/NDP verhouding (elastisiteite was tussen -0.31 en -0.50).

Summary

Fermentation in *Zymomonas mobilis* has been described as a catabolic highway, with 50 % of soluble protein comprising glycolytic and fermentative enzymes. In conjunction with one of the fastest observed fermentations, the conversion of glucose to ethanol forms one of the least efficient energy extractions found in nature. The low energy yield of fermentation in *Z. mobilis* is a result of the usage of the Entner-Doudoroff glycolytic pathway, which has half the energy yield per mol substrate compared to the well known Embden-Meyerhof-Parnas glycolytic pathway.

The work presented in this thesis forms part of a larger project to compare glycolytic regulation in different micro-organisms (i.e., *Z. mobilis*, *Escherichia coli, Saccharomyces cerevisiae* and *Lactococcus lactis*). These organisms were chosen based on their usage of different glycolytic mechanisms. By using supply-demand analysis for quantifying glycolytic regulation as well as similar experimental conditions (e.g. using non-growing cell cultures), we can compare the regulatory behaviour of mechanistically distinct free-energy supplies.

The aim of this thesis was to quantify the importance of anaerobic free-energy generation for the regulation of the Entner-Doudoroff glycolytic pathway in *Z. mobilis*. We used metabolic control analysis (MCA) and supply-demand analysis to realize this goal. The central message of MCA is that when a metabolic parameter (e.g., a conserved metabolic moiety) is deemed important for affecting a particular steady-state variable (i.e., fermentation flux), its effect on the steady state variable should be tested. An extension to MCA, supply-demand analysis, provides a quantitative framework for analyzing the regulatory importance of cellular commodities such as anaerobic free-energy. This is done through comparing the elasticities of anaerobic free-energy supply and demand, which yields the degree to which the respective reaction blocks control the flux through anaerobic free-energy metabolism, as well as determine the cellular free-energy state (ATP/ADP ratio).

The regulation of anaerobic free-energy metabolism in *Z. mobilis* was investigated with an experimental approach. The key features of our experimental setup were the use of NMR spectroscopy for detecting metabolites, as well as employing non-growing conditions for supply-demand experiments. With NMR spectroscopy metabolites could be detected in real time without using invasive sampling techniques; the use of non-growing conditions further simplified the analysis by enabling us to correlate fermentative behaviour exclusively with the anaerobic free-energy state.

Fermentation of glucose was investigated in the wild type *Z. mobilis*, a recombinant containing a non-expressing plasmid, or expressing plasmids for over-expressing the glucose facilitator (TCDB 2.A.1.1.4) or glucose-6-phosphate dehydrogenase (EC 1.1.1.49). In addition, ATP demand in the non-expressing recombinant and wild type was perturbed by titrating with the uncoupler acetic acid. Our results show that the anaerobic free-energy demand, the glucose facilitator and glucose-6-phospate dehydrogenase all control the flux of ethanol production in *Z. mobilis*. The Entner-Doudoroff glycolytic supply activity was found to be sensitive to changes in the ratios of ATP/ADP (elasticity varied between –0.31 and –0.49) and NTP/NDP (elasticity varied between –0.31 and –0.50).

Opgedra aan my Ouers – dankie vir die ondersteuning en opoffering

Acknowledgements

Prof JM Rohwer: **Prof** thanks for the opportunity to study under your supervision. While your expert guidance was always a source of direction, I was allowed the freedom to explore my own ideas. Your faith in me was invaluable in making this thesis a success.

Prof JL Snoep: Your expert guidance was a driving force in making this thesis a success.

Arrie Arends: A lab manager that makes a large contribution to the enjoyable research experience the JJJ-lab offers.

Jean McKenzie, Elsa Malherbe, Arno Hanekom and Dr DJ Brand: Four people that enthusiastically share their NMR spectroscopy expertise. **Jean** your execution of the flux determinations during the first 2 supply-demand experiments was highly satisfactory and greatly appreciated.

Dr R Conradie: **Riaan** thanks for your friendship and sporadic provision of shelter (often longer than planned). Your interest and critical discussions regarding the content of this thesis are greatly appreciated. I also want to thank you as well as **Kora Holm** for translating the thesis summary into Afrikaans.

Dr CM Malherbe: Your HPLC expertise is greatly appreciated.

JJJ-lab students: For continual contributions to the work presented in this thesis. I specifically want to thank **Justin Smith, Sandra Jordaan** and **Johann Eicher** who through their similar research experience made a large contribution to the work presented in this thesis. Further thanks to **Gerald Penkler** and **Francois du Toit** for respectively assisting with spectrophotometric analysis and helping with the preparation of figures.

NRF (National Research Foundation): For funding.

Contents

Chapter 1

Introduction

1.1) General Remarks

Zymomonas mobilis is an obligatory fermentative bacterium occurring in sugar rich environments (1). The conversion of glucose to ethanol forms the major metabolic pathway in *Z. mobilis*, with glycolytic and fermentative enzymes constituting half of soluble protein (2). The high glycolytic and fermentative enzyme levels lead to near maximal ethanol yields (i.e., 2 mol of ethanol per mol glucose consumed), as well as one of the fastest fermentations known in the microbial world (3). The strong fermentative capacity is accompanied by inefficient ATP production, i.e., $Y_{ATP/Glucose}$=1 (mol ATP produced per mol glucose consumed) under anaerobic conditions, which is explained by the usage of the Entner–Doudoroff glycolytic pathway. Figure 1.1 compares the ATP yields of the Entner–Doudoroff glycolytic pathway and the well known Embden–Meyerhof–Parnas glycolytic pathway, as well as the enzyme differences which are restricted to the hexose-phosphate part of glycolysis (4). Since the Entner-Doudoroff pathway is usually associated with aerobes, it is unique that this pathway functions as primary energy source under anaerobic conditions in *Z. mobilis* (4). The unique energy metabolism of *Z. mobilis* provides an excellent experimental model for investigating the control[1] and regulation[2] of the Entner-Doudoroff glycolytic pathway. The energy metabolism of *Z. mobilis* will be discussed in Section 1.3.

[1] Metabolic control: The responsiveness of metabolic variables (i.e., metabolites or fluxes) following
[2] Metabolic regulation: The maintenance of metabolic homeostasis in the face of varying cellular demands.

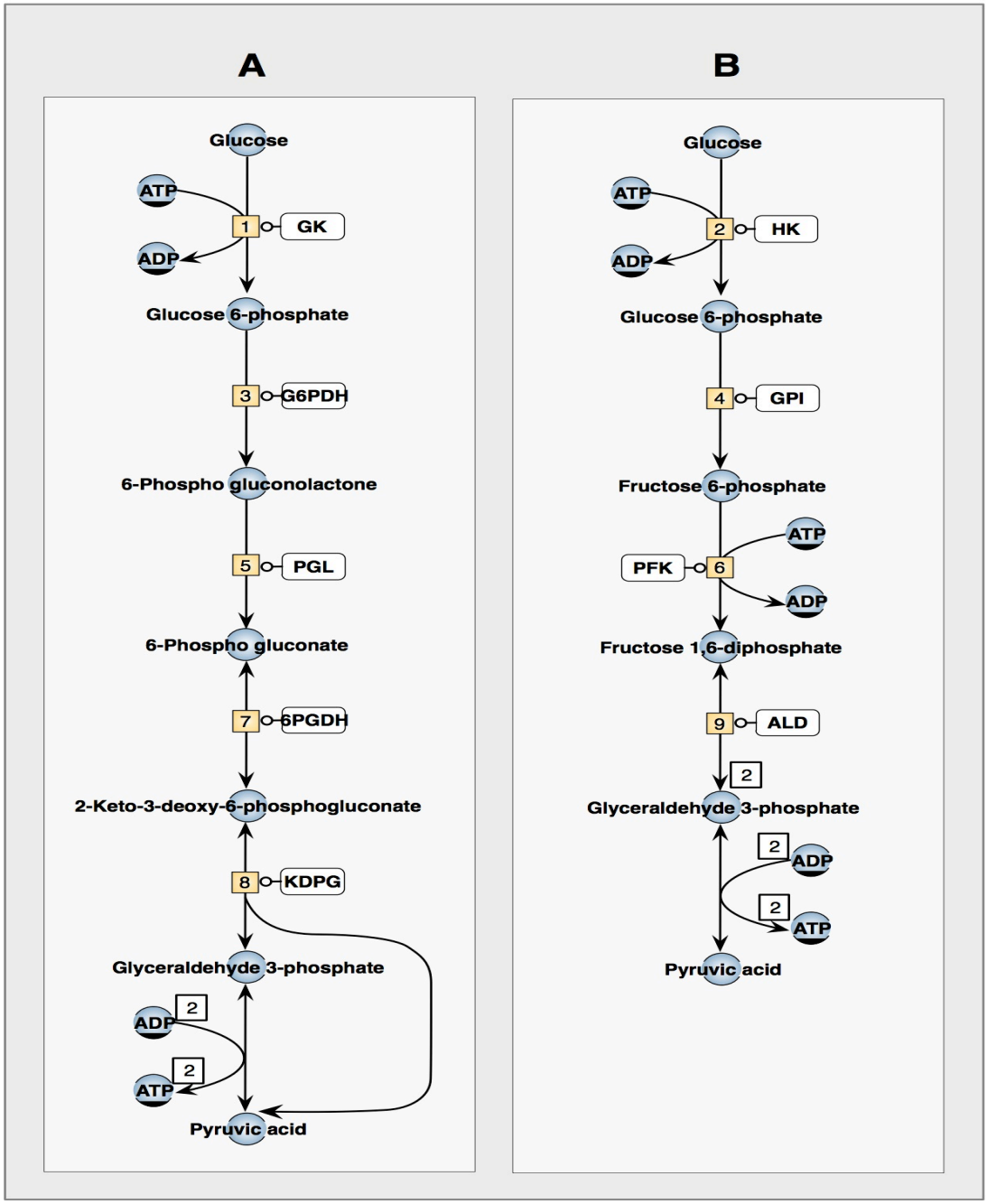

Fig. 1.1 Comparison of the Entner-Doudoroff glycolytic pathway with the Embden-Meyerhof-Parnas glycolytic pathway.

Abbreviations: A, Entner-Doudoroff pathway; B, Embden-Meyerhof-Parnas pathway; Numbers: (1), glucokinase (EC 2.7.1.2); (2), hexokinase (EC 2.7.1.1); (3), glucose-6-phosphate dehydrogenase; (4), glucose phosphate isomerase (EC 5.3.1.9); (5), phosphogluconolactonase (EC 3.1.1.31); (6), phosphofructokinase (EC 2.7.1.11); (7), 6-phosphogluconate dehydratase (EC 4.2.1.12); (8), 2-keto-3-deoxy-6-phosphogluconate aldolase (EC 4.1.2.14); (9), aldolase (EC 4.1.2.13)

Two schools of thought have primarily been used to investigate the control and regulation of glycolysis in *Z. mobilis*. The first school of thought, the 'rate-limiting theory', advocates that slow enzymes limit metabolism during times of excess (i.e., slow glycolysis when ATP levels are high), and through their pacemaker potential (cooperative enzyme properties) are able to respond to changing demand (5, 6). The *Z. mobilis* glycolytic enzymes glucose-6-phosphate dehydrogenase and phosphoglycerate mutase (EC 5.4.2.1) have been identified in this manner as possible regulatory enzymes (7). The study used quantitative NMR spectroscopy to show that glucose 6-phosphate and 3-phosphoglycerate are at higher levels than the rest of the glycolytic intermediates. Therefore according to the 'rate-limiting theory' the enzymes catalyzing the conversion of glucose 6-phosphate and 3-phosphoglycerate to their respective products are slow compared to the rest of the enzymes in *Z. mobilis* glycolysis.

The second school of thought centres on investigating metabolism as an interacting system. This is brought about by the knowledge that metabolism is constituted of thousands of interacting components, and that these interactions are important when investigating metabolic control and regulation. Metabolic control analysis (MCA), which will be discussed in Section 1.4, is a systems biology framework, which was developed to study the steady-state behaviour of metabolism quantitatively (7, 8). This allows comparison of the control by different enzymes and furthermore provides quantitative coefficients for relating local properties (i.e., enzyme properties) to systemic properties (i.e., fluxes and steady-state concentrations). MCA has been used to investigate glycolytic control in *Z. mobilis*, with the glucose facilitator, glucokinase and glucose-6-phospate dehydrogenase shown to have control over glycolytic flux (3).

By regarding the glycolytic pathway as a component of metabolism, it becomes clear that glycolytic behaviour is not only influenced by its constituents, but also by the connections it forms with other parts of metabolism. The regulatory importance of these connections can be investigated with supply-demand analysis, which is an extension of MCA, (9). Supply–demand analysis states that the regulatory importance of a component should be assessed by considering its functional relationship with metabolism, and will

also be further discussed in Section 1.4. Since energy availability is a necessity for cellular viability, the regulatory performance of anaerobic glycolysis should be assessed in terms of anaerobic energy production and consumption. Such an analysis has not yet been conducted for *Z. mobilis*.

Apart from anaerobic energy production, glycolysis provides precursors for anabolic processes and is coupled, under aerobic conditions, to aerobic energy metabolism through the citric acid cycle and the electron transport chain. The multifunctional nature of glycolysis complicates control analysis, since all the functions influence its behaviour. It was therefore important for this investigation to simplify fermentative complexity in order to correlate glycolytic behaviour with only the anaerobic cellular energy state. *Z. mobilis* converts up to 97 % of glucose to equimolar mixtures of ethanol and CO_2 under anaerobic conditions, suggesting almost exclusive coupling through anaerobic energy with the rest of metabolism (10). Fermentative coupling with anabolism can be further reduced by investigating glycolytic control under non-growing conditions, which prevents the utilization of pathway intermediates for biosynthesis (11). Therefore, the regulatory importance of anaerobic energy can be determined by refining the connections glycolysis has with the rest of metabolism.

Nuclear Magnetic Resonance (NMR) is a spectroscopic technique that exploits the magnetic properties of atoms for the purpose of molecular structure determination and quantification of molecular concentrations. NMR detects nuclei with uneven proton-numbers and/or uneven neutron-numbers, including ^{31}P and ^{13}C, popular nuclei used to investigate metabolic behaviour. The main advantage of investigating glycolytic regulation with NMR is the ability to detect metabolite progression in real time, without using invasive sampling techniques (i.e., *in vivo* measurement) (12). Furthermore, pre-selection of metabolites is not necessary, which can lead to the detection of unsuspected metabolites. This is illustrated by an NMR study on *Z. mobilis* fermentation extracts which yielded UTP levels that exceeded ATP levels (13). For these reasons NMR is an ideal technique to unravel the importance of anaerobic energy generation for the regulation of the Entner-Doudoroff glycolytic pathway in *Z. mobilis*. A drawback of

NMR spectroscopy is its insensitivity, which is evident by the difficulty to resolve or detect *in vivo* NDP (nucleoside di-phosphate) for most bacterial studies (14). NMR spectroscopy is further discussed in Section 1.5.

1.2) Aim and outline of thesis

The **aim** of this thesis was to assess the flux control distribution between anaerobic free energy supply (glycolysis) and demand (non-growing energy demand), as well as the respective reaction block contribution to anaerobic free energy homeostasis.

The **outline** of this thesis is as follows. The rest of Chapter 1 discusses energy metabolism in *Z. mobilis*, supply-demand analysis and *in vivo* NMR spectroscopy. Chapter 2 focuses on the experimental design and preliminary control experiments for supply-demand analysis, while Chapter 3 gives the results of the experimental supply-demand experiments. Chapter 4 is a general discussion of the work done in this thesis, with Chapter 5 summarizing the experimental procedures.

1.3) Energy metabolism in *Z. mobilis*

The gram-negative facultative anaerobic bacterium *Z. mobilis* is prevalent in sugar rich environments such as ripening honey, sugarcane- and palm sap. These environments are rich in glucose, fructose and sucrose; the exclusive fermentable substrates of *Z. mobilis* (1). In this section the mechanisms used for extracting energy from fermentable sugars, the sole use of facilitated diffusion to assimilate hexose-sugars, and the mechanism used for osmo-protection are discussed.

The osmo-protecting periplasmic enzyme glucose-fructose oxidoreductase (EC 1.1.99.28), as well as the exclusive usage of facilitated diffusion (uniport) to assimilate glucose (K_M 2–4 mM) and fructose (K_M 40 mM) are metabolic features known amongst prokaryotes only in *Z. mobilis* (10, 15, 16). Glucose-fructose oxidoreductase plays an essential role in the survival of *Z. mobilis* in extra-cellular sugar environments which are

hypertonic (17, 18). It catalyzes with very low affinity the conversion of fructose to sorbitol (K_M 400 mM, glucose-fructose oxidoreductase is a ping-pong enzyme with glucose providing the electrons), which is transported into the cytoplasm to counteract dehydration (19, 20). While hypertonic extra-cellular environments put osmotic constraints on cellular viability, the energy potential of the naturally occurring sugar concentration gradient is harnessed through energy independent assimilation of fermentable substrates. Non-fermentable sugars such as mannose (K_M 8mM) and xylose (K_M 40 mM) are also assimilated, which could furthermore play an auxiliary role in protecting *Z. mobilis* against dehydration (19). Sucrose, the third fermentable substrate of *Z. mobilis*, is hydrolyzed to glucose and fructose by periplasmic levansucrase (EC 2.4.1.10) enzymes before assimilation and fermentation (levansucrase enzymes transfer the fructose moiety of sucrose to polyfructose (or levan), with concomitant release of glucose, Ref 21).

Z. mobilis uses a linear constitutive version of the Entner-Doudoroff glycolytic pathway to catabolize glucose and fructose. Other organisms also utilize this pathway, with *E. coli* containing a linear inducible version and *Pseudomonas* a cyclic version (4). We restrict our discussion to the Entner-Doudoroff glycolytic pathway as it occurs in *Z. mobilis*. The conversion of 1 mol hexose to 2 mol pyruvate yields 1 mol ATP, which, in conjunction with the fermentative enzymes pyruvate decarboxylase and alcohol dehydrogenase, is probably the least efficient fermentative energy extraction found in nature (4, 22). The low energy yield of the Entner-Doudoroff pathway is caused by aldolase activity yielding 1 mol glyceraldehyde-3-phosphate per mol hexose consumed, and not two, as is the case with the Embden-Meyerhof-Parnas glycolytic pathway (refer to Figure 1.1). The fate of pyruvate, the other three carbons yielded by the Entner-Doudoroff 2-keto-3-deoxy-6-phosphogluconate aldolase reaction, is ethanol fermentation.

Over-expression of the Entner-Doudoroff glycolytic enzymes glucose-6-phosphate dehydrogenase, glucokinase and the glucose facilitator lead to stimulation of fermentation flux (3). Growth assessment of *Z. mobilis* recombinants with increased fermentative performance has been consistent with the observation that growth is not

coupled to ATP production, i.e., compared to the wild type $Y_{Biomass/ATP}$[3] decreases for the recombinants (3, 23). *Z. mobilis* therefore demonstrates uncoupled growth, which is a phenomenon where energy production is not coupled to the energy required for growth (23). The rapid catabolic flux of *Z. mobilis*, which leads to energy production that exceeds growth requirements, has been explained in terms of the low energy yield ($Y_{ATP/Glucose}$) of the Entner-Doudoroff pathway, the high expression levels of glycolytic and fermentative enzymes, as well as the hypothesized absence of fermentative control based on the absence of phosphofructokinase (1, 10, 23, 24). While high enzyme levels and inefficient energy extraction ($Y_{ATP/Glucose}$) are pertinent features of *Z. mobilis* fermentation, they do not suffice in explaining the maintenance of rapid catabolic flux (23). That is, ADP needs to be stoichiometrically regenerated during fermentation even if this ATP demand is not met by the energy required for growth (under anaerobic conditions *Z. mobilis* fermentation is stoichiometrically completely coupled to the *general* ATP demand). Further evidence supporting uncoupled growth in *Z. mobilis* is given by its low growth yield ($Y_{Biomass/ATP} = Y_{Biomass/Glucose}$[4] = 2.3-10.5) in comparison with other organisms, as well as decreased growth yield in conjunction with increased fermentative productivity under acidic conditions (pH 4 versus pH 6.5); non growing *Z. mobilis* cultures consume glucose at high specific rates (approximately 0.42 μmol glucose.min^{-1}.mg dry^{-1} weight observed for this study.) (23). Note that under non-growing conditions growth and ATP production are energetically completely uncoupled ($Y_{Biomass/ATP} = Y_{Biomass/Glucose} = 0$). Energetic uncoupling should however not be confused with stoichiometric coupling, which is independent of any specific ATP demand.

Optimal functioning of fermentation requires the constant cycling of conserved metabolic moieties. The almost complete conversion of glucose to ethanol and CO_2 by *Z. mobilis* under anaerobic conditions shows NAD(P) moiety cycling to be solely dependent on the glycolytic and fermentative enzymes. The cycling of nucleoside phosphates is however not clear, since as discussed in the previous paragraph, the energy requirements for growth are too low to account for total ATP consumption. For the regeneration of ADP,

[3] Biomass produced (gram) per mol ATP produced.
[4] Biomass produced (gram) per mol glucose consumed.

other ATP consuming reactions have been proposed, with the primary candidate being the membrane F_0F_1-type H^+-ATPase (EC 3.6.3.14; Ref. 25, 26). It has been proposed that the F_0F_1-type H^+-ATPase is responsible for up to 20 % of the total ATP turnover (26, 27).

The F_0F_1-type H^+-ATPase proposed for playing a key role in maintaining rapid fermentation flux is a true H^+-ATP synthase (23). This enzyme, in conjunction with all the membrane components needed for electron transport, provides *Z. mobilis* with all the metabolic requirements necessary for oxidative phosphorylation (23). Furthermore, while *Z. mobilis* is an obligatory fermentative organism respiratory rates comparable to the fastest oxygen-consuming microorganisms are achieved under aerobic cultivation (23). However, respiration in *Z. mobilis* does not facilitate growth as is common for most facultative anaerobic organisms (28, 29). For *Z. mobilis* there seems to be a 'tug of war' between fermentation and respiration, with the outcome for aerated cultures a sharing of reducing power (both pathways consume NADH), which leads to the toxic accumulation of fermentative acetaldehyde as there is insufficient NADH for its complete reduction to ethanol. This ultimately reduces the growth rate (23). Therefore the energy producing potential of respiration, as illustrated under non-fermentative conditions through extra-cellular acidification or ethanol feeding, seems to be offset by its disruptive effect on fermentative moiety conservation (the cycling of ATP and ADP is exclusively dependent on the glycolytic and fermentative enzymes; Ref 11, 29); extra-cellular acidification facilitates trans-membrane translocation of protons by the F_0F_1-type H^+-ATPase, while the conversion of ethanol and NAD^+ to acetaldehyde and NADH by alcohol dehydrogenase (EC 1.1.1.1) provides reducing power for the electron transport chain).

1.4) Supply-demand analysis

Metabolism can be viewed as a cellular economy where pathways either produce or consume cellular commodities such as amino acids and energy equivalents (ATP, Ref 9). An example of metabolic organization where production and consumption pathways are linked by a cellular commodity is the non-growing anaerobic energy metabolism of *Z. mobilis*. Under these conditions energy supply and biomass production are energetically

completely uncoupled ($Y_{Biomass/ATP}$ = 0), making the anaerobic cellular energy state (ATP/ADP) the sole linkage between fermentation and the non-growing energy demand. Fermentation is therefore functionally completely defined in terms of its connection with the rest of metabolism.

According to the theory of supply-demand analysis the functional performance of supply and demand reaction blocks can be helpful to understand metabolic control (9). A functional performance of metabolism can be assessed by plotting the respective sensitivities (defined below) of supply and demand pathways toward the metabolite that links them on a combined rate characteristic (9). By using the visual approach of combined rate characteristics in combination with MCA, the degree to which the respective reaction blocks control the flux through the reaction system, as well as determine the magnitude in which the linking metabolite varies, can be assessed (9). Supply-demand analysis has shown that when one reaction block completely controls the flux through the reaction system, the other block completely determines the degree of homeostatic maintenance of the linking metabolite. Such a reaction system is functionally differentiated in that the respective reaction blocks either control flux or determine linking metabolite homeostasis.

MCA, the method on which supply-demand analysis is based, is well suited for investigating the functional performance of metabolism since the degree to which local metabolic parameters (i.e., enzyme concentrations and the conserved sum of moiety-conserved cycles) control the systemic steady-state behaviour or variable properties of metabolism (i.e., fluxes and metabolite concentrations at steady state) can be assessed (7, 8). Note that the identity of variables and parameters depends on the timeframe of the metabolic events under consideration, which is subject to experimental verification (for example the time-frame in which enzyme levels remain constant is organism and condition-specific). The dependency of metabolic variables on reaction activities is described by the control coefficient (C_v^y), and is defined as the percentage change in any metabolic variable (y) following a one percent change in the activity of a reaction step

(v). Since MCA deals with the steady state condition, the reference as well as the perturbed systemic position needs to be at steady state.

$$C_v^y = \frac{d \ln y}{d \ln v} \tag{1.1}$$

While control coefficients give information about the systemic behaviour of metabolism, the elasticity coefficient (ε_s^v), a local property, describes how sensitively the rate (v) of a reaction responds to a one percent change in the level of an effector (s) interacting directly with it. To determine a particular elasticity for, say, S, the other metabolites are kept at their respective steady state levels.

$$\varepsilon_s^v = \frac{\partial \ln v}{\partial \ln s} \tag{1.2}$$

Before considering the relation between elasticities and control coefficients let us consider an enzyme-catalyzed coupled reaction where the substrate (s) is converted via the linking metabolite (x) to product (d) (A coupled reaction is used to explain MCA, because exactly the same type of analysis will apply for supply-demand analysis). For our example (s) and (d) are fixed while $v(\text{supply})$, the rate at which (s) is converted to (x), is at steady state equal to $v(\text{demand})$, the rate at which (x) is converted to (d). Furthermore, the net reaction direction is from left to right.

$$s \xrightarrow{v(\text{supply})} x \xrightarrow{v(\text{demand})} d$$

Fig. 1.2 Two coupled enzyme-catalyzed reactions.

The control properties of the reaction system with respect to the metabolite (x) and the flux (J) through the reaction system obey the following relationships (7, 8).

$$C^{J}_{v(\text{supply})} + C^{J}_{v(\text{demand})} = 1 \tag{1.3}$$

$$C^{x}_{v(\text{supply})} + C^{x}_{v(\text{demand})} = 0 \tag{1.4}$$

These are the summation theorems for flux and concentration control coefficients, which state that the flux control coefficients (C^{J}_{v}) of all enzymes affecting a particular metabolic flux (J) add to one and all concentration control coefficients (C^{x}_{v}) of enzymes affecting a particular metabolite (x) add to zero. The systemic behaviour of the reaction system can be related to its local properties through the flux connectivity property and concentration connectivity property (Equations 1.5 and 1.6 respectively), which describe how the elasticities, $\varepsilon^{v(\text{supply})}_{x}$ and $\varepsilon^{v(\text{demand})}_{x}$, relate to the control coefficients (9).

$$C^{J}_{v(\text{supply})}\varepsilon^{v(\text{supply})}_{x} + C^{J}_{v(\text{demand})}\varepsilon^{v(\text{demand})}_{x} = 0 \tag{1.5}$$

$$C^{x}_{v(\text{supply})}\varepsilon^{v(\text{supply})}_{x} + C^{x}_{v(\text{demand})}\varepsilon^{v(\text{demand})}_{x} = -1 \tag{1.6}$$

By using the connectivity and summation theorems the control coefficients of the reaction system can be written in terms of elasticities (9).

$$C^{J}_{v(\text{supply})} = \frac{\varepsilon^{v(\text{demand})}_{x}}{\varepsilon^{v(\text{demand})}_{x} - \varepsilon^{v(\text{supply})}_{x}} \tag{1.7}$$

$$C^{J}_{v(\text{demand})} = \frac{-\varepsilon^{v(\text{supply})}_{x}}{\varepsilon^{v(\text{demand})}_{x} - \varepsilon^{v(\text{supply})}_{x}} \tag{1.8}$$

$$C^{x}_{v(\text{supply})} = -C^{x}_{v(\text{demand})} = \frac{1}{\varepsilon^{v(\text{demand})}_{x} - \varepsilon^{v(\text{suppply})}_{x}} \tag{1.9}$$

The control analysis of a simple coupled reaction provides a framework for analyzing more complicated reaction networks in a similar fashion. To illustrate this let us consider the reaction scheme in Figure 1.3 where reactions one to six catalyze the conversion of (*a*) to (*f*). For the reaction system (*a*) and (*f*) are fixed while the rates of the individual reactions are equal, i.e., the reaction system is at steady state. As previously, the net reaction direction is considered from left to right.

$$\overset{v(\text{supply})}{(a \leftrightarrow b \leftrightarrow c \leftrightarrow)} x \overset{v(\text{demand})}{(\leftrightarrow d \leftrightarrow e \leftrightarrow f)}$$

Fig. 1.3 A linear enzyme-catalyzed reaction sequence. Reactions are grouped into supply and demand blocks as indicated by parentheses.

There are primarily 2 opposing strategies for analyzing the control of the reaction sequence depicted in Figure 1.3. The first, a bottom-up approach which would be similar to the analysis for the reaction scheme in Figure 1.2, would focus on how individual reactions determine the steady state behaviour of the reaction system. The second, top-down metabolic control analysis, aims to simplify control analysis by grouping reactions into producers and consumers of a linking metabolite (in practice this is done to negate the inherent complexity of reaction systems or when little is known about a particular reaction sub-system, Ref. 30). By treating the reaction sequence as a coupled reaction, the control properties of the reaction system can be described in terms of the elasticities of the supply and demand reaction blocks (note that the elasticities of supply and demand are the respective combined responses of the individual reaction blocks toward the clamped linking metabolite; from the definition of elasticities (Equation 1.2) the linking metabolite becomes the parameter of the reaction sub-system). Therefore a top-down control analysis for the reaction sequence depicted in Figure 1.3, where reactions one to

three are the producers of (x) and reactions four to six are the consumers of (x), yields the same relationships between control coefficients and elasticity coefficients as Equations 1.7–1.9.

The usage of MCA in combination with rate characteristics sets supply-demand analysis apart from top-down control analysis, since it shows the behaviour of supply and demand in response to changes in the linking metabolite over a wide concentration range (9, 30). Figure 1.4 shows the usage of combined rate characteristics for supply and demand, and the point where the rate characteristics intersect yields the steady state level of (x) and the steady state flux (J). The elasticities of supply and demand are calculated as the respective slopes $\frac{\partial \ln v(\text{supply})}{\partial \ln x}$ and $\frac{\partial \ln v(\text{demand})}{\partial \ln x}$ at the intersection points. From the elasticities the control properties of the reaction scheme in Figure 1.3 can be calculated by using Equations 1.7 - 1.9.

Control analysis of supply and demand reaction blocks, whether the blocks represent single or multiple reactions, can show how the functions of flux control and metabolite homeostasis are distributed between these reaction blocks. Apart from the algebraic approach (Equations 1.7 - 1.9) a visual approach can be used to assess functional differentiation, with the values of the supply and demand elasticities at the steady state point determining the magnitude of the steady state variation in (J), on the y-axis, and the magnitude of the linking metabolite (x) variation, on the x-axis, in response to a perturbation. Therefore a visual picture of how the values of the elasticities determine the control structure of the supply-demand reaction system can be attained (for detailed discussions of the visual approach to assess functional differentiation refer to Ref. 9). From both approaches it can be concluded that primary flux control resides in the reaction block with the lowest elasticity, while the block with the highest numerical

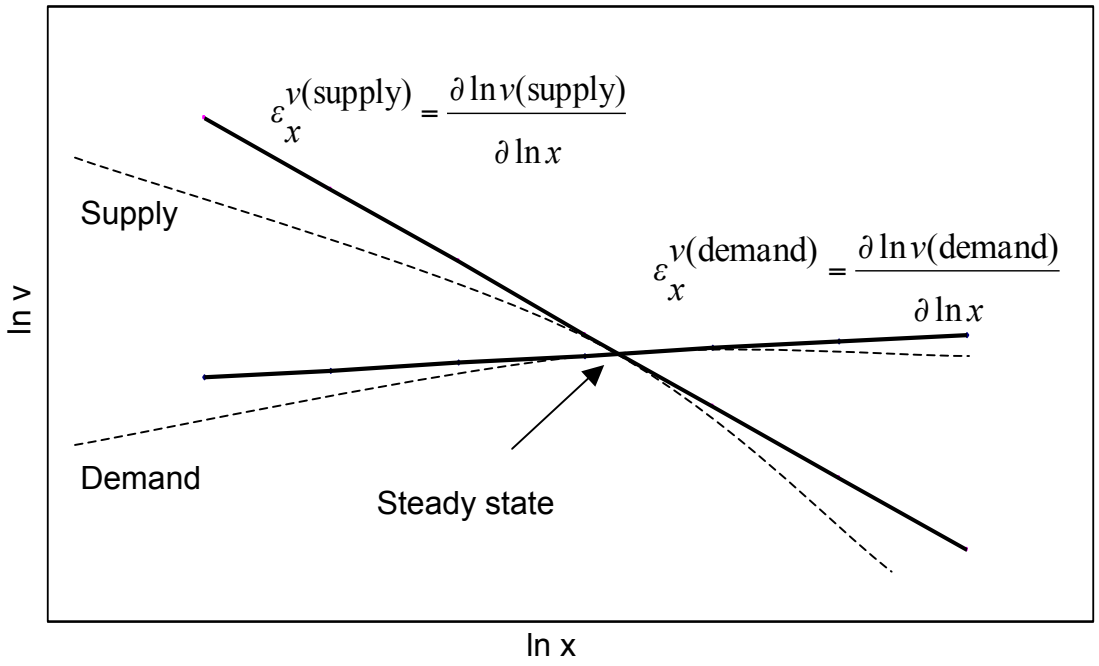

Fig. 1.4 Rate characteristics of supply and demand (dotted lines). The elasticities of supply and demand (solid lines) at the steady state point are roughly based on values obtained for an *E. coli* anaerobic free energy experimental analysis, where fermentation was the anaerobic free energy supply and free energy consumption the anaerobic free energy demand (to keep with the flow of this section the respective captions of the linking metabolite on the x-axis, and supply and demand fluxes on the y-axis were kept generic, Ref. 31). The numerical values of the supply and demand elasticities are respectively -1 and 0.1. From equations 1.7 – 1.8 the flux control coefficients of supply and demand are respectively 0.1 and 0.9. From equation 1.9 the concentration control coefficients of supply and demand are respectively 0.9 and -0.9. Therefore 90% of flux control resides in the demand, with the supply making the largest contribution to linking metabolite homeostasis.

elasticity makes the greater contribution in determining the magnitude of the variation in the linking metabolite. Furthermore, when one block has an elasticity value of zero it has total flux control, and in turn the elasticity value of the other block then completely determines the magnitude of the variation of the linking metabolite. Such a supply-demand reaction system would be completely functionally differentiated, in that both

reaction blocks have independent functions which are either flux control or determining the magnitude of the variation of the linking metabolite.

Supply-demand analysis quantifies the control and emphasizes the regulatory importance of a cellular commodity (i.e., a so-called "linking" metabolite). By considering the thousands of metabolic components, their interactions, and time-variant behaviour, it becomes clear that deciding which linking metabolite to investigate is difficult. While supply-demand analysis does not give rigorous guidelines regarding the choice of linking metabolite, it provides a clear quantitative framework in which the regulatory significance of linking metabolites can be assessed. Furthermore an extension to supply-demand analysis, coined generalized supply-demand analysis, has been developed to remove investigator bias regarding the choice of linking metabolite, allowing comparison of the regulatory significance (e.g. in terms of functional differentiation) of all the metabolites in a reaction system (32). The manner in which the regulatory importance of linking metabolites is tested does not only follow a top-down approach, but combines it with a bottom-up approach as follows. Each variable metabolite is fixed in turn, and varied above and below its steady state concentration, allowing construction of rate characteristics for comparing the responses of enzymes directly attached to metabolites (elasticity coefficients) with the response of supply and demand reaction blocks (response coefficients). Furthermore when the behaviour of a reaction block shows similar kinetic behaviour as a component enzyme, the agreement provides evidence that the linking metabolite is an important controller. Generalized supply-demand analysis is a computational approach and thus only applicable to kinetic models of pathways.

1.5) *In vivo* Metabolomics with Nuclear Magnetic Resonance Spectroscopy

To account for the chemical, mechanical and interactive constraints of the cellular environment, *in vivo* cell physiological investigations aim to study cellular events as they occur. NMR is well suited for investigating physiology in the cellular environment, because the different chemical natures of various metabolites gives rise to unique

magnetic properties that can be exploited with spectroscopy in a non-invasive non-destructive manner (12, 33).

NMR spectroscopy involves studying the interaction of electromagnetic radiation with matter; particularly the interaction of radio waves with atomic nuclei immersed in an external magnetic field (12, 33). Certain atomic nuclei (with uneven proton-numbers and/or neutron-numbers) when placed in an external magnetic field can be exploited with spectroscopy, because the magnetic field-induced energy differences between nuclear spin-states allow for the absorption of electromagnetic energy. This absorption of precise amounts of electromagnetic energy brings about NMR. The amounts of electromagnetic energy required to bring about NMR depends on the interplay between the magnetic moment of the nucleus under investigation and the strength of the external magnetic field. For example for a 600 MHz NMR spectrometer the proton will bring about NMR at a radio wave frequency of 600 MHz (NMR spectrometer-magnet strengths are named according to the electromagnetic radiation energy requirements to bring about NMR for the proton) (12, 33). Therefore for the same magnetic field strength, nuclei with smaller magnetic moments, for example phosphorus and carbon, would require radio waves with a lower frequency to bring about NMR. While different nuclei require different amounts of energy to bring about NMR, nuclei of the same type might also require varying degrees of electromagnetic energy to bring about NMR (12, 33). This happens when nuclei of the same type differ in terms of their attached chemical groups. For example for acetic acid the methyl carbon and carboxyl carbon will have differential electron densities, leading to dissimilar local magnetic properties, and ultimately unique energy requirements to bring about NMR. The specific NMR frequencies at which nuclei absorb energy (due to electronic shielding) are the basis for resolving atoms in the same molecule and atoms in different molecules. These energy differences are however much smaller than those between different types of nuclei and are presented in a dimensionless manner, i.e., ppm (parts per million): $(\nu_{reference}-\nu_{sample})/(\nu_{sample}) * 10^6$, where $\nu_{reference}$ is the NMR frequency (Hz) of a reference nuclide and ν_{sample} the NMR frequency (Hz) of a nuclide of interest. The expression of NMR frequencies in ppm is called chemical shift.

Detection of NMR signals is possible because it involves studying nuclear populations and thus measuring the signal emanating from large numbers of nuclei at the same time. Figure 1.5 shows the theoretical behaviour of 2 million proton nuclei at 18.8 Tesla (magnetic field strength). The small discrepancy between the 2 possible proton spin populations leads to an energy difference, which was discussed in the previous paragraph allows for the absorption of precise amounts of electromagnetic energy. Physically the energy absorbed induces nuclear flipping between the 2 spin states, with the high energy spin state becoming more populated. This happens because the low energy spin state is originally more populated, which increases the probability of flipping to the high energy spin state. NMR occurs during this redistribution of nuclear spins, which are detected through the voltage induced by the absorbed energy. There are two important factors for the quantitative detection of NMR signals. Firstly, the spin systems should be relaxed since the voltage signal after a pulse is dependent on the energy absorbed by the original unperturbed spin system. This is particularly relevant for pulsed NMR spectroscopy which uses multiple pulses to improve the signal to noise ratio (not allowing for sufficient relaxation causes saturation). Secondly, an internal standard should be used since only a fraction of the nuclear spins is detected.

The magnetized induced separation of nuclear spins gives rise to nuclear coupling, which can be observed as peak splitting in NMR spectra. Just as the electron densities of NMR receptive nuclei cause chemical shift through local magnetic influence, the nuclear spins of neighbouring NMR receptive elements also influence the specific frequency at which NMR will occur. However the dual nature of the nuclear spin states (high or low energy spin states for spin ½ nuclei such as ^{13}C, ^{31}P, ^{1}H) causes variable magnetization, and therefore variable energy requirements to attain NMR – ultimately leading to peak splitting. The splitting patterns of resonances can be complicated, which can be simplified by using ^{1}H decoupling. This involves applying strong electromagnetic pulses (at the specific frequency of ^{1}H) to equalize ^{1}H spin populations; ultimately making ^{1}H 'not NMR receptive'.

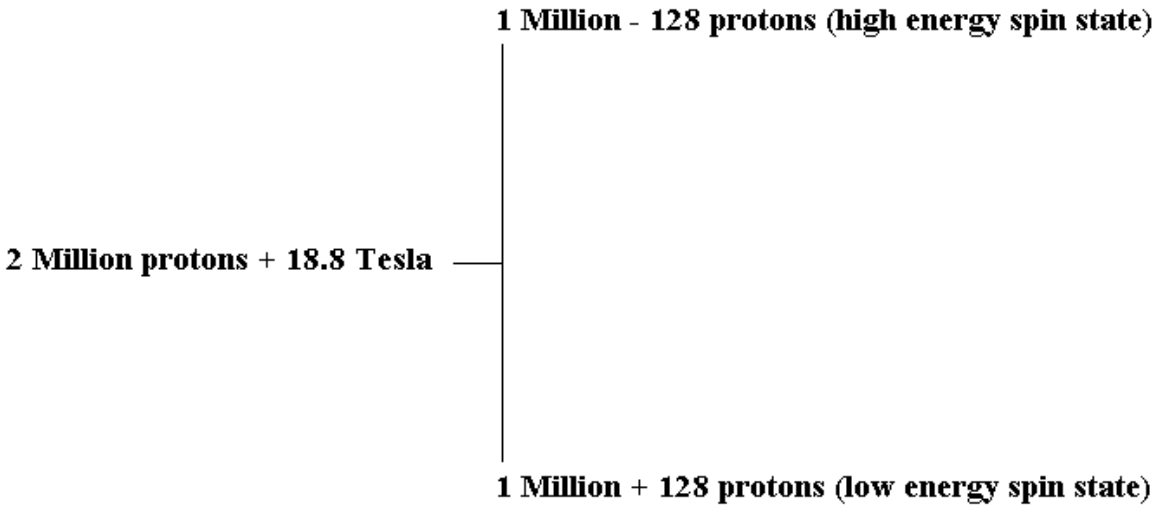

Fig. 1.5 The magnetized induced separation of nuclear spin states for ^{1}H (spin quantum number = ½) at 18.8 Tesla. The theoretical relative populations were calculated using the Boltzmann equation (34). This figure was adapted from (34).

While nuclei might possess the necessary physical properties to bring about NMR, the manner in which they occur *in vivo* needs to be considered when attempting to detect metabolites. The detection of metabolites with NMR spectroscopy is therefore subject to *in vivo* constraints, for example the low levels of some metabolic intermediates might be too low for detection, or metabolites bound to proteins or paramagnetic ions might cause broadening of signals, and ultimately peak-overlap or the inability to detect signals. To overcome the constraints of the cellular environment, strategies such as extraction, chemical shift reagents and other biological considerations such as increasing the sampling time by prolonging active metabolism and thus improving signal quality, can be employed. Furthermore, sensitivity, abundance and spectral resolution need to be considered when choosing the type of nuclei for analysis:

- Sensitivity is proportional to the magnetic moment of a nucleus, with protons having the largest magnetic moment, and carbon nuclei the smallest of the three nuclei discussed.
- Increased natural abundance enhances NMR signal strength, with ^{1}H and ^{31}P 100% abundant and ^{13}C only 1.1%.

- Spectral resolution is dependent on the susceptibility of the electron density surrounding the nucleus, with ^{13}C the most susceptible.

The generally low levels of ^{31}P in cells restrict the number of intermediates that can be quantified with ^{31}P NMR spectroscopy. The carbon isotope that is NMR active is less abundant as well as less sensitive, compared to the proton and phosphorus nuclei, but has a wider window for spectral resolution. Also, it allows specific spiking with ^{13}C-labelled substrates, which enhance the NMR signal.

NMR has been successfully employed to study the metabolism of *Z. mobilis*. Barrow *et. al.* (13) used *in vivo* NMR to investigate intracellular pH and metabolic control, and also quantified glycolytic intermediates. Surprisingly it was found that UTP exceeded ATP levels. The same authors also investigated the stereo-specificity as well as mechanisms of glycolytic enzymes, with one of the findings the preferential usage of the ß anomer of D-glucopyranose by *Z. mobilis* glycolysis (35). A particular advantage of using NMR to investigate metabolism is the ability to capture metabolic events in short time domains, i.e., milliseconds. Schoberth *et. al.* (36) made use of this property to investigate the rate of ethanol diffusion across the plasma membrane. Finally a flow-through NMR system was developed by De Graaf *et. al.* (14) to compare glucose, fructose and xylose metabolism. From a NMR sensitivity perspective it was the first time *in vivo* NDP was detected and quantified in *Z. mobilis*.

By following metabolic progression in real time with NMR spectroscopy, difficulties with choosing extraction procedures that will not interfere with *in vivo* metabolite levels are overcome. Furthermore, under conditions where metabolites and fluxes can be measured simultaneously, a complete *in vivo* picture of the variable properties of metabolism can be generated.

The preceding sections provided background information regarding our aim of studying the importance of anaerobic energy generation for the control of the Entner-Doudoroff glycolytic pathway in *Z. mobilis* with supply-demand analysis and *in vivo* NMR

spectroscopy. In Chapter 2 the experimental design as well as control experiments for supply-demand analysis are discussed.

Chapter 2

Experimental design and preliminary experimental controls

2.1) Experimental design

Supply-demand analysis of anaerobic energy metabolism, where anaerobic fermentative energy production is the supply and energy consuming reactions constitute the demand, requires measurement of the flux responsiveness of the respective reaction blocks toward the anaerobic cellular energy state. Experimentally this is done through the independent modulation of the supply or demand reaction block, with concomitant measurement of the effect on the ATP/ADP ratio, as well as the flux of the non-modulated reaction block. The double-modulation method can therefore serve as a direct experimental application for supply-demand analysis (37).

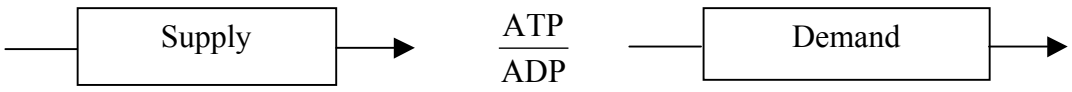

Fig. 2.1 Supply and demand communicating exclusively through the ATP/ADP ratio under anaerobic conditions (38).

2.1.1) Modulating the supply

Z. mobilis recombinants containing separate plasmids for overexpressing glucose–6–phosphate dehydrogenase and the glucose facilitator were used to modulate the energy supply. The genes on these plasmids are inducible, with IPTG (isopropyl-β-D-1-thiogalactopyranoside) relieving the *lacI*^{q} induced repression of the *tac* promoter. However in the absence of IPTG the *lacI*^{q} gene product represses the *tac* promoter only partially, leading to leaky expression of genes on these plasmids. This leaky expression

enhances fermentative performance, with further induction usually not improving fermentation performance (3, 39). For a detailed discussion of the construction of *Z. mobilis* expression plasmids refer to (40, 41).

2.1.2) Modulating the demand

In the absence of growth dependent energy expenditure under non-growing conditions, incremental acidification of the cytoplasm was used to modulate the energy demand (through addition of 2 mM, 5mM, 10mM and 20mM acetate). As discussed in Section 1.3, it is proposed that 20 % of the ATP turnover in *Z. mobilis* is driven by a trans-membrane F_0F_1-type H^+-ATPase-dependent futile proton cycle. Acetic acid, possibly through increasing F_0F_1-type H^+-ATPase activity, has been shown to have a de-energizing effect on *Z. mobilis* (42, 43). The de-energizing effect of acetic acid is pH-dependent, with acidity facilitating protonation and therefore movement through the hydrophobic cell membrane into the cytoplasm (acetic acid pK_a = 4.75). While acidity facilitates movement into the intra-cellular environment, the more basic cytoplasmic environment (pH 6.4) enhances acetic acid dissociation and therefore energy expenditure by the F_0F_1-type H^+-ATPase to counter acidification of the cytoplasm (13). The effect of cytoplasmic acidification on glycolytic and fermentative enzymes was not investigated in this thesis. The fate of intra-cellular acetic acid is unsure.

2.2) Preliminary experimental controls

The experimental design requires that supply and demand communicate exclusively through the anaerobic cellular energy state for reference and modulated states. This allows determination of the elasticity values of supply and demand towards the anaerobic cellular energy state. Furthermore, while the high extra-cellular levels of glucose and ethanol simplify *in vivo* flux measurement, difficulty with *in vivo* detection of intra-cellular anaerobic free energy intermediates required the preparation of cell free extracts. Nevertheless, there was good reason for using NMR here as well. As mentioned in Chapter 1, NMR spectroscopy does not require the pre-selection of the analyte, as is

required e.g. for enzymatic analysis. Figure 2.7 below shows that this enabled us to identify and quantify uridine nucleotides in the same experiment where adenylates were determined, which in all eventuality would not have been picked up by specific directed enzymatic assays.

Finally, enzyme activity was determined to verify plasmid dependent over-expression of glycolytic enzymes in recombinants, which were used for the supply modulations. This required optimization of a sonication procedure for preparation of cell-free extracts.

2.2.1) Limiting cellular energy production to anaerobic fermentation

To limit the communication between the supply and demand blocks to the adenine nucleotides, *Z. mobilis* was pre-grown under anaerobic conditions, and non-growing conditions were used for supply-demand analysis. These strategies were used to prevent biosynthesis and respiration from influencing fermentative behaviour, with the stoichiometric oxidation of glucose to ethanol rendering fermentation exclusively responsive to the anaerobic free energy state.

$$\text{Glucose} + ADP + P_i \rightarrow 2\text{Ethanol} + 2CO_2 + ATP$$

Fig. 2.2 The net reaction for anaerobic glucose fermentation in *Z. mobilis*.

2.2.1.1) Fermentation product analysis with HPLC

The fermentation product analysis of the wild type *Z. mobilis* and recombinants, illustrated in Figure 2.3, shows that within experimental error almost all glucose (100 mM) was converted to ethanol. The levels of acetate and glycerol were also very low, which is in agreement with the high ethanol yields. Therefore non-growing fermentation product analysis with HPLC shows that *Z. mobilis* was producing ATP solely by the Entner-Doudoroff pathway in both the reference and modulated states.

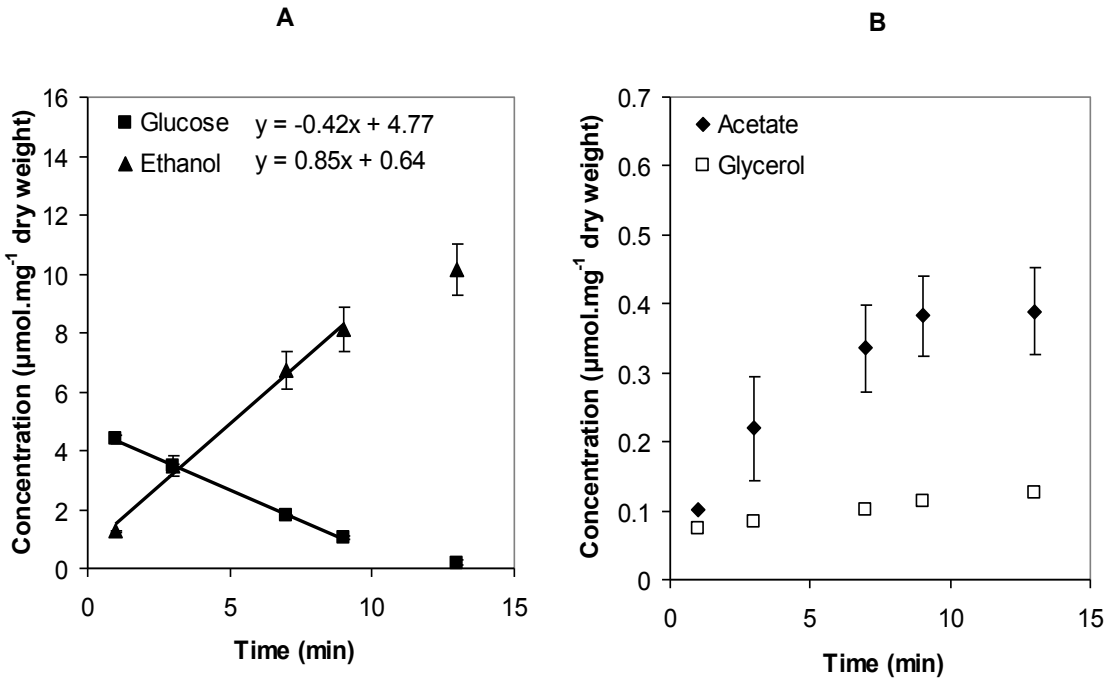

C

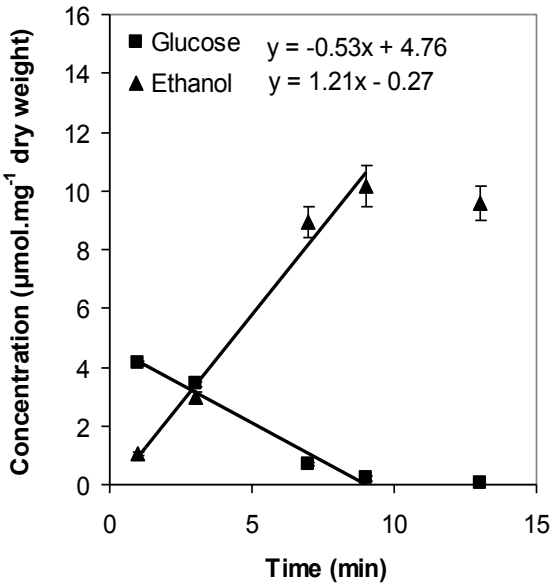

D

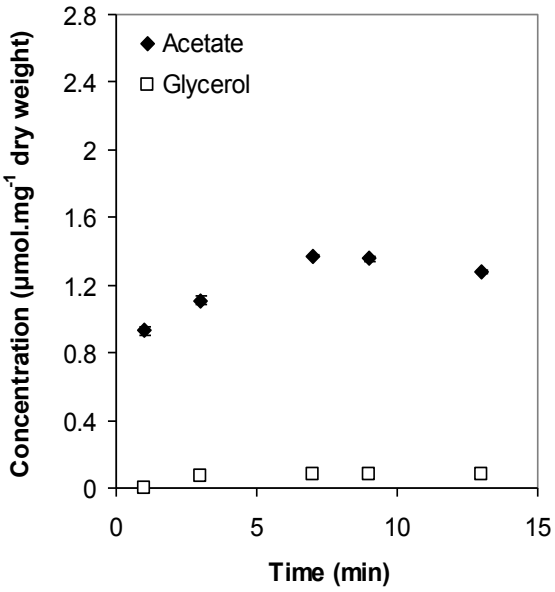

E

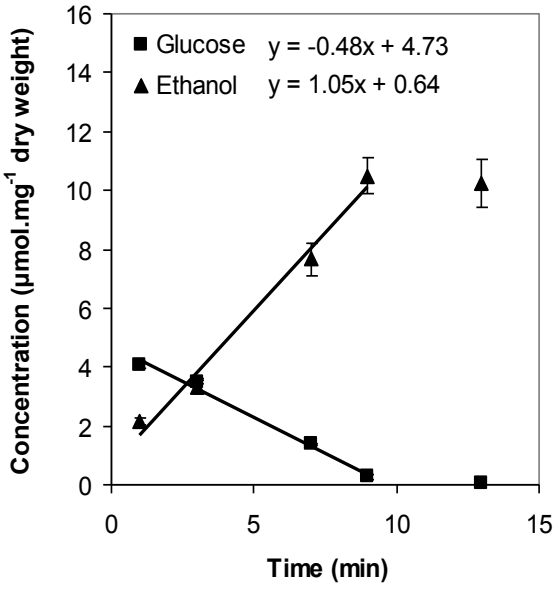

F

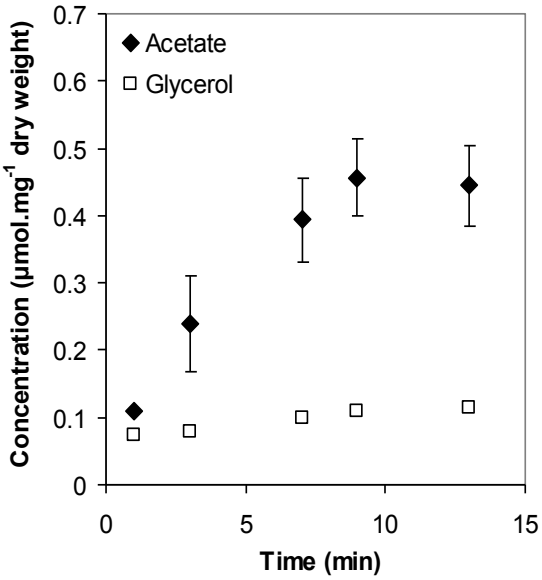

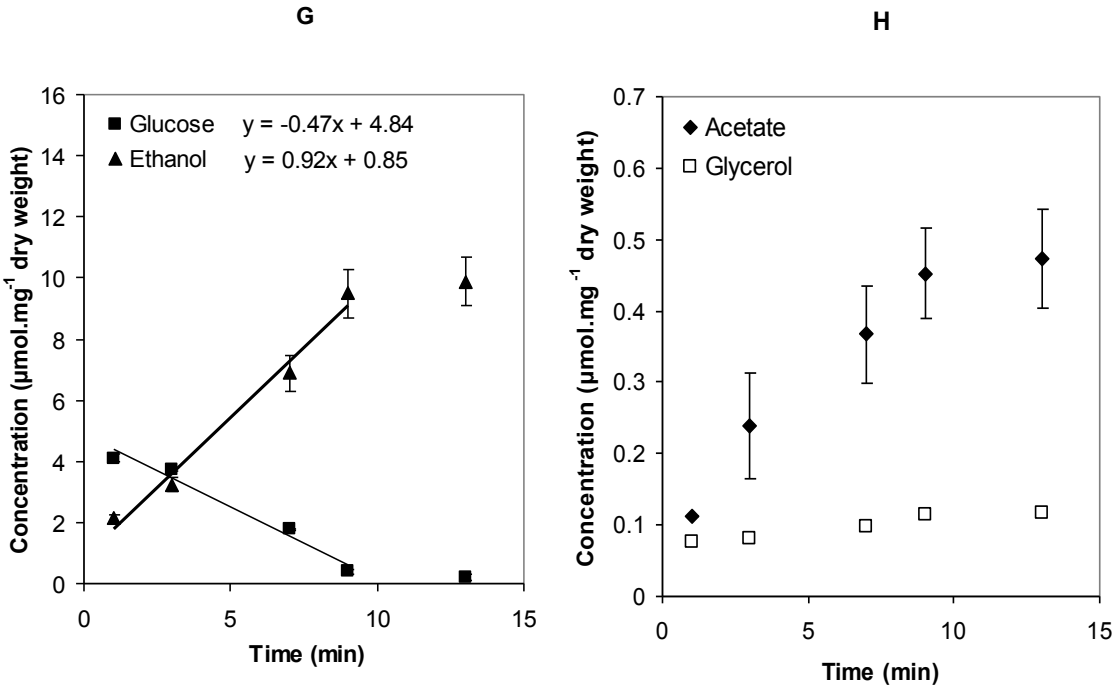

Fig. 2.3 Fermentation profiles of the recombinants used for the supply modulations, as well as the most extreme demand modulation, 20 mM acetate in the wild type, were analyzed with HPLC (cell density OD_{550} = 100, 100 mM glucose (4.72 µmol.mg^{-1} dry weight), 30 ^{o}C). The respective fermentation profiles are shown for the wild type (A & B), the wild type with addition of 20mM acetate (C & D), the recombinant containing plasmid for over-expressing glucose-6-phosphate dehydrogenase (E & F), and the recombinant containing plasmid for over-expressing the glucose facilitator (G & H). Error bars indicate SEM of the glucose, ethanol and acetate time courses (*n*=2). In some cases the error bars are hidden behind the data points. The lines and equations indicate linear regression used for calculating glucose and ethanol fluxes. Averaged dry weight values obtained during previous OD_{550} = 100 (21.18 mg/ml dry weight; SEM=0.58 *n*=18) experiments were used for normalizing fluxes.

2.2.1.2) Fermentation product analysis with NMR spectroscopy

A *Z. mobilis* recombinant containing a non-expressing plasmid was also used during the supply-demand analysis. As was the case with the wild type and over-expressing

recombinants, energy metabolism was investigated through fermentation product analysis (Section 2.2.1.1). While HPLC was used previously, *in vivo* ^{13}C NMR spectroscopy was used for the non-expressing recombinant. The results indicate that almost all glucose was converted to ethanol (discussed below).

In order to overcome the low sensitivity of NMR spectroscopy (which is caused by the small energy differences between magnetized induced nuclear spin states), high cell densities had to be used for detection of metabolic intermediates, which led to an experimental setup where glucose was rapidly consumed (10-12 min, as is evident from the HPLC fermentation product analysis in Figure 2.3). Since cell free extracts were used for measuring metabolic intermediates with ^{31}P NMR, the short time-frame of active fermentation did not place time constraints on data acquisition. However the need to synchronize the time-frame of metabolic events during preparation of cell free extracts with metabolic events during *in vivo* measurement of fluxes, required us to use rapid pulse sequences for flux measurement to gain sufficient signal to noise ratio within a suitably short time scale. This led to saturation of carbon nuclei (the frequency at which radio waves were applied to the fermentation sample was faster than the time it took for ^{13}C nuclei to relax from NMR). The following paragraphs discuss procedures for determining glucose and ethanol levels from saturated glucose and ethanol ^{13}C-NMR resonances.

The spectra in Figure 2.4 were collected after glucose depletion to determine saturation of ethanol resonances (*in vivo* ^{13}C NMR). In 2.4 (A) a short recycle delay was used (0.35 s) with the spectrum in 2.4 (B) collected under relaxed conditions (15 s recycle delay). Quantification of carbon resonances originating from MES-buffer showed that its peak intensities remained similar under rapidly pulsed and relaxed conditions (i.e., MES carbon resonances were relaxed under both conditions); making it possible to visualize ethanol saturation through comparison with MES-buffer peak intensities. Under saturated conditions the methyl group of ethanol (peak 6) was 3.60 (SEM=0.10, n=4) times smaller compared to relaxed conditions; this factor was used to scale ethanol resonances.

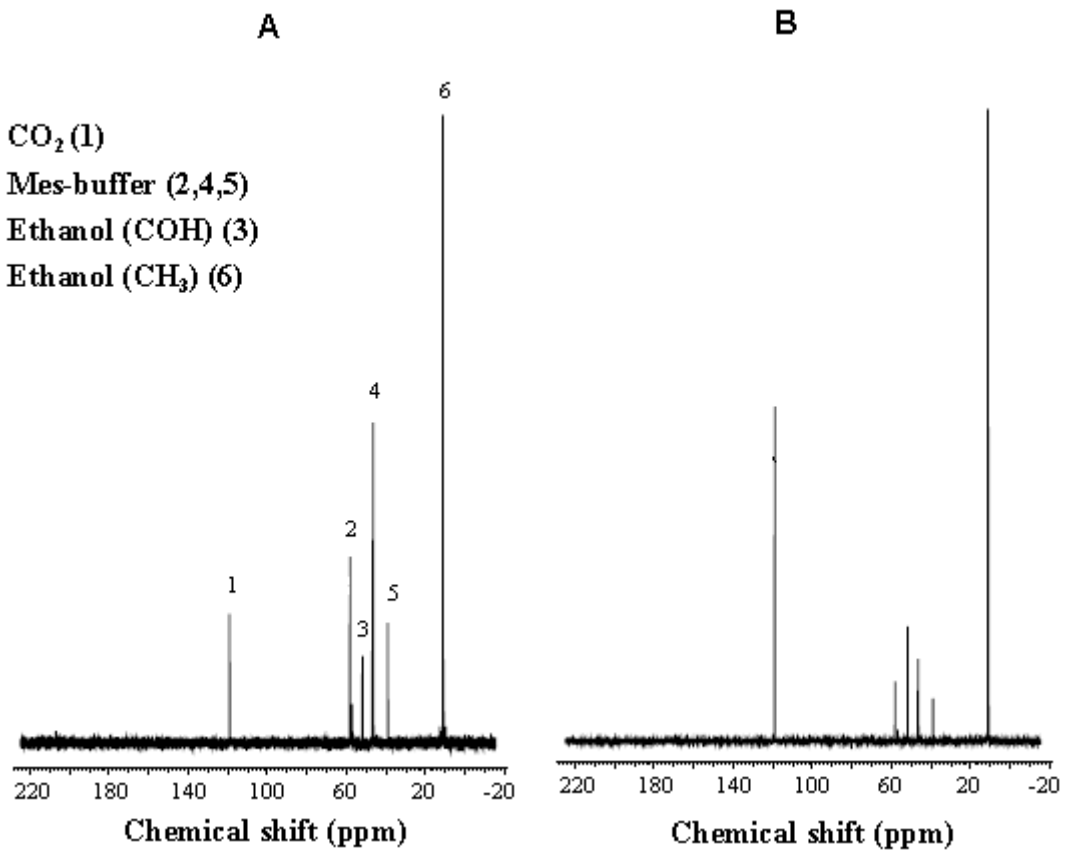

Fig. 2.4 *In vivo* ^{13}C NMR spectra collected after glucose depletion used for determining an ethanol saturation factor. The cell density was OD_{550} = 75 with 78 mM glucose (of which 10.5 mM was [1,6-$^{13}C_2$]) added. *In vivo* ^{13}C NMR spectra were measured on a Varian 600 MHz spectrometer with the following pulse parameters: pulse duration (12 µs), flip angle (90^o), acquisition time (0.65 s), broadband ^1H decoupling (0.65 s during acquisition time), (A) pre-acquisition time (0.35 s), (B) pre-acquisition time (15 s). The other parameters were as described in Chapter 5.

Since relaxed conditions were used during collection of the spectrum in 2.4 (B), the ethanol yield from glucose can be calculated directly; respectively yielding 88 % (SEM=0.03, *n*=4) and 88 % (SEM=0.03, *n*=4) conversion to the hydroxyl and methyl carbons of ethanol. Note that the comparatively larger methyl carbon resonance of ethanol is caused by the incorporation of carbon six from ^{13}C labelled glucose [1,6-$^{13}C_2$]

(carbons 2 and 5 of glucose yield the hydroxyl carbon of ethanol with carbons 3 and 6 yielding the methyl carbon; carbons 1 and 4 of glucose yield carbon dioxide).

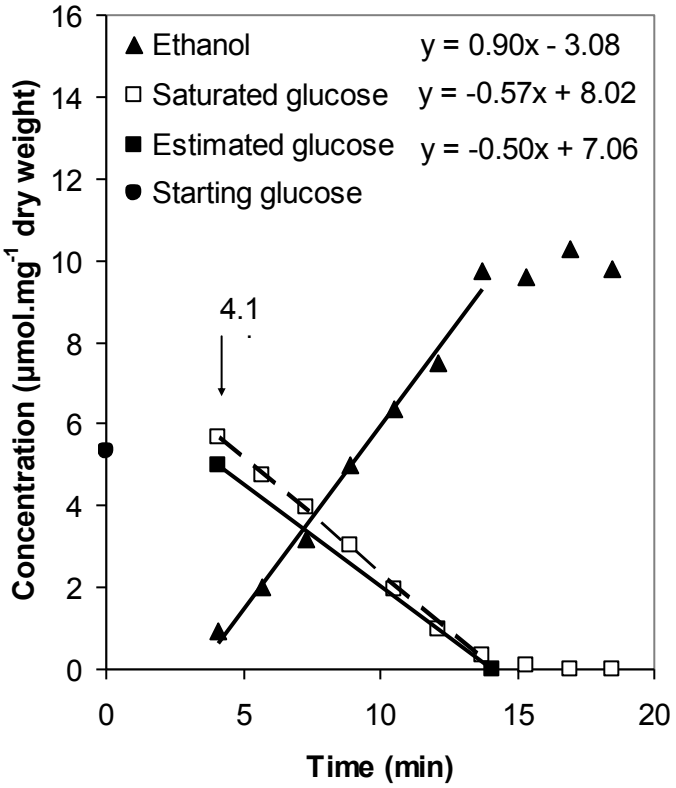

Fig. 2.5 Fermentation profile of the *Z. mobilis* recombinant CP4 + pLOI706EH (containing a non-expressing plasmid) analyzed with *in vivo* ^{13}C NMR. The cell density was OD_{550} = 75 with 78 mM glucose (of which 10.5 mM was [1,6-$^{13}C_2$]) added. The lines and equations indicate linear regression used for calculating glucose and ethanol fluxes. The glucose flux was 0.51 umol.min^{-1}.mg^{-1} dry weight (SEM=0.01, *n*=2), with the ethanol flux 0.92 umol.min^{-1}.mg^{-1} dry weight (SEM=0.02, *n*=2); which corresponded to 90 % conversion of carbons 3 and 6 of glucose to the methyl group of ethanol. Averaged dry weight values obtained during previous OD_{550} = 75 (14.60 mg/ml dry weight; SEM=0.06 *n*=9) experiments were used for normalizing fluxes. The cellular volume (4.38 % (V/V)) was estimated by using the conversion factor 3 µl.mg^{-1} dry weight, which was important for determining the concentration of the internal standard (MES-buffer, not transported into the cytoplasm, Ref. 36).

Figure 2.5 shows glucose and ethanol fluxes calculated from saturated *in vivo* ^{13}C NMR spectra. To obtain ethanol fluxes the methyl carbon resonances were scaled by a factor 3.60 to compensate for saturation (as discussed in previous paragraph). Ethanol levels were further scaled to convert detectable carbon (^{13}C, 1.1 % natural abundance) to total carbon. Glucose fluxes were estimated; they could not be measured accurately since rapid *in vivo* glucose consumption made determination of an experimental saturation factor difficult (refer to Figure 2.4). Estimation of glucose fluxes centred on determining the glucose level at the start of steady state consumption (time-point 4.1 min), as well as the duration of complete steady state consumption. The glucose level at time-point 4.1 min was calculated from the corresponding ethanol level (as determined from a linear fit through the steady state ethanol production) by using the fermentation stoichiometry obtained in Figure 2.4 (88 %). This yielded an estimated glucose flux of 0.51 $\mu mol.min^{-1}.mg^{-1}$ dry weight, compared to 0.53 $\mu mol.min^{-1}.mg^{-1}$ dry weight if 100 % conversion were used in the calculation. Finally the duration of complete steady state consumption was determined from a linear fit through the steady state saturated glucose data (dotted line in Figure 2.5).

2.2.2) Measuring the anaerobic cellular energy state

Even with flow-through ^{31}P NMR, an *in vivo* based extension to NMR spectroscopy that allows for increased accumulation time and therefore better signal quality, detection of the anaerobic cellular energy state in *Z. mobilis* was limited to NTP and NDP (14). Our own efforts to detect and quantify NTP and NDP also centred on increasing the accumulation time and therefore improving the signal to noise ratio. We used a batch-type NMR experimental setup, and increased the accumulation time by using higher starting glucose levels, as well as decreasing the fermentation temperature to prolong active fermentation. These efforts were, however, unsuccessful, necessitating the use of extraction techniques as an alternative strategy to quantify the nucleotides. Extracted samples can in principle be analysed as long as needed on the NMR spectrometer; this enabled the quantification of NTP and NDP due to improved signal-to-noise ratios. While extraction has draw-backs in terms of not accounting for the cellular environment, it does

allow for resolving the different types of nucleoside phosphates, a feat currently not possible with *in vivo* ^{31}P NMR (14).

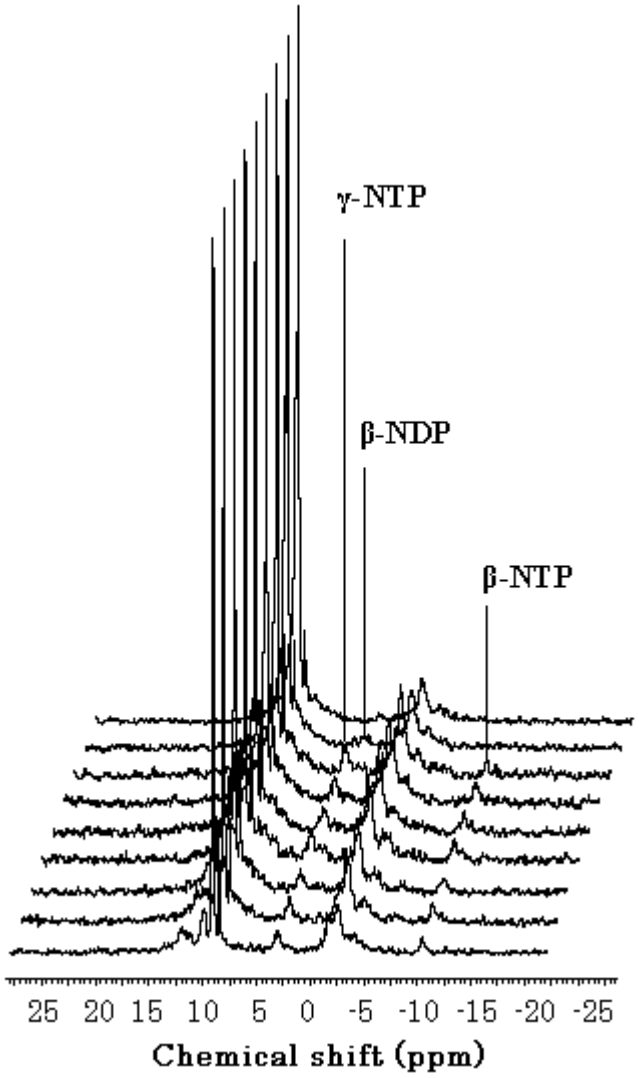

Fig. 2.6 Stack plot of *in vivo* ^{31}P NMR spectra collected at 242 MHz, with a time-resolution of 1 min per spectrum during glucose fermentation by *Z. mobilis*. The cell density was OD_{550} = 400 (approximately 80 mg/ml dry weight) with 250 mM glucose added at 30 ^{o}C. The NMR parameters are described in Chapter 5.

Figure 2.6 shows *in vivo* ^{31}P NMR spectra collected during glucose fermentation. The first 7 spectra show through visual inspection a relatively constant NTP level, which might even be at steady state, the metabolic state required for MCA. However for the same spectra NDP was either absent or very inconsistent, rendering *in vivo* ^{31}P spectra unsuitable for determining the anaerobic cellular energy state and therefore supply-demand analysis. The inability to resolve NTP and NDP or even detect NDP could be caused by factors that restrict their mobility, which is a prerequisite for liquid state NMR spectroscopy. These factors could include binding to enzymes or paramagnetic ions, or the viscous nature of the cytoplasm, ultimately leading to NMR signal-broadening. Extracting NTP and NDP from the cellular environment, as well as further sample clarification, led to ^{31}P NMR spectra with finer resonances as can be seen by comparing Figure 2.6 with Figure 2.7.

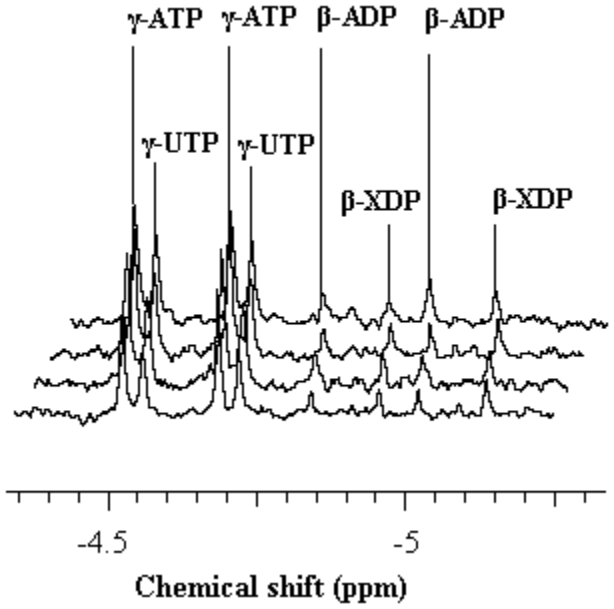

Fig 2.7 Example of extracts made during the fermentation (5 min – 8 min) of glucose by *Z. mobilis* (CP4) and analyzed with ^{31}P NMR spectroscopy. Spectra were accumulated at 121 MHz for 3 h per spectrum and are clipped to focus on the nucleoside phosphates. Standard NMR parameters for extracts as described in Chapter 5 were used. Abbreviation: β-XDP, unidentified β-nucleoside di-phosphate.

Peaks in Figure 2.7 were identified through addition of pure standards, except for XDP (unidentified nucleoside di-phosphate) which was tentatively assigned through spin-coupling and chemical shift similarities with ADP. The NTP and NDP doublets are caused by ^{31}P-coupling. Physically the β-ADP - α-ADP ^{31}P-coupling can be understood in terms of their spin states. The application of external magnetization causes net spin and therefore the existence of dual spin-states in the case of ^{31}P, which leads to both nuclei 'experiencing' variable magnetization; and ultimately splitting of both resonances into two components. The multiplicity rule ($2nI + 1$) can be used to assist with predicting the splitting patterns of nuclei, and states that the number of components into which a resonance splits is dependent on the number of nuclei (n) interacting with it as well as their spin quantum number (I, which equals ½ for ^{31}P; Ref. 12, 33). By focusing on the β-ADP ^{31}P nuclide, only elements closer than four bonds are considered for coupling. Since broadband ^{1}H decoupling was employed during data acquisition, protons can be ignored as elements contributing to splitting. ^{17}O and ^{13}C do not have enough magnetization to detectably split the β-ADP phosphate resonance (^{17}O natural abundance = 0.037 %, ^{13}C natural abundance = 1.1 %). This leaves only the α-ADP ^{31}P nuclide (natural abundance of 100 %) able to cause splitting, and according to the multiplicity rule the β-ADP phosphate resonance split into 2 components.

The advantage of using extraction for supply-demand analysis is the ability to resolve the different nucleoside phosphates, therefore being able to focus on the adenylate anaerobic cellular energy state as the link between supply and demand. However, it also provides the opportunity to ask 'what if' questions regarding the significance of the other nucleoside phosphates for controlling the cellular free-energy state. In Figure 2.7 the UDP level dropped below detection during active fermentation, making the combined NTP/NDP ratio (ATP+UTP)/(ADP+XDP) an alternative anaerobic cellular energy ratio to compare with the ATP/ADP ratio.

2.2.3) Optimization of a sonication procedure for preparation of cell free extracts

Z. mobilis recombinants containing plasmids for over-expressing the glucose facilitator and glucose-6-phosphate dehydrogenase were used to modulate the anaerobic free energy supply. To verify whether plasmid incorporation indeed led to enzyme over-expression, a sonication procedure for preparation of cell free extracts was optimized for determining enzyme activity (to quantify the levels of enzyme over-expression). Figure 2.8 shows that after 3.25 min of intermittent sonication all the cells were broken and the NADH production rate remained constant. Glucose-6-phosphate dehydrogenase was used as an assay example, with the reaction constituting the conversion of glucose 6-phosphate and NAD^+ to 6-phospho-gluconolactone and NADH.

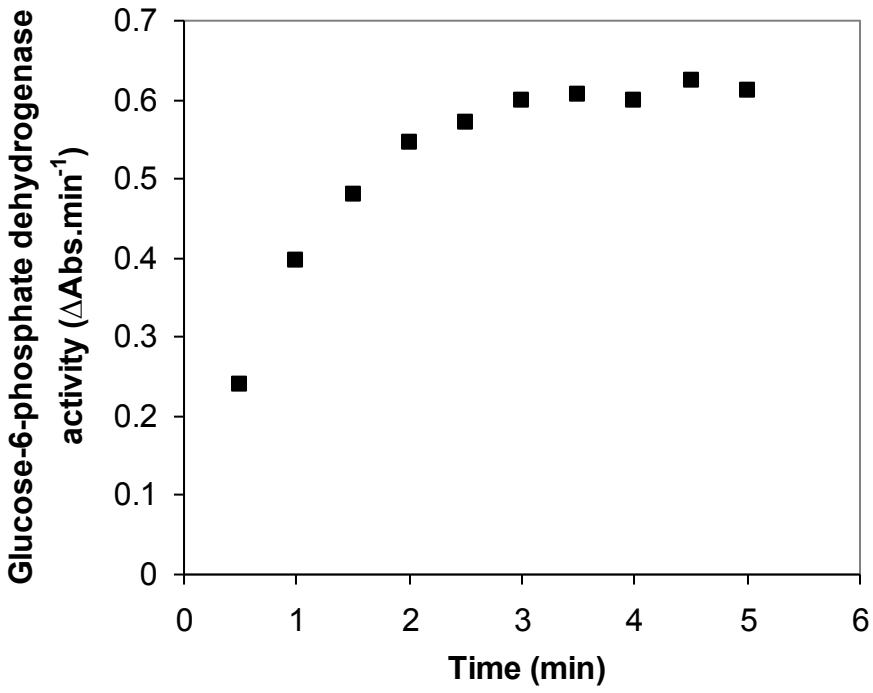

Fig. 2.8 The NADH production rate measured at 340 nm as a function of sonication time. Glucose-6-phosphate dehydrogenase was used as an assay example, with NAD^+ and glucose 6-phosphate added to the cell extract and determining activity over 30 s.

Chapter 2 summarized the verification of the experimental design for anaerobic supply-demand analysis around the free-energy metabolites ATP and UTP. Methods for measurement of the anaerobic cellular energy state were developed, and a protocol for preparation of cell free extracts was optimized to verify plasmid dependent over-expression of enzymes by recombinants. The following chapter summarizes the results of the experimental supply-demand analysis.

Chapter 3

Experimental supply-demand analysis

Supply-demand analysis of anaerobic energy metabolism under fermentative conditions requires measurement of the flux responsiveness of the supply and demand reaction blocks toward the anaerobic cellular energy state. Experimentally this is done through the independent modulation of the supply and demand reaction blocks, by measuring the effect on the ATP/ADP ratio as well as on the flux through the non-modulated reaction block. Since the reactions that constitute the non-growing energy demand were not all known in detail, we obtained their flux by measuring the glycolytic flux, and assuming that it equalled the demand flux because the ATP/ADP ratio was at steady state. This was possible because the steady-state supply of free energy came almost exclusively from the Entner-Doudoroff glycolytic pathway (as verified with the HPLC and *in vivo* ^{13}C NMR fermentation product analysis in Chapter 2), enabling us to equate glycolytic flux with ATP synthesis flux.

3.1) Flux control by supply and demand over glucose consumption and ethanol production

The effect of over-expressing glucose-6-phosphate dehydrogenase (CP4 + pLOI711, modulating the supply – refer to ZWF in figures), as well as simultaneous modulation of supply and demand (CP4 + pLOI711 + 25 mM acetate respectively) on glucose consumption and ethanol production are shown in Figure 3.1. Compared to the reference state (CP4, wild type *Z. mobilis*), over-expression of glucose-6-phosphate dehydrogenase led to an increased specific glucose consumption rate, as well as a small increase in the specific ethanol production rate. Simultaneous modulation of supply and demand had a small effect on the glucose consumption rate and a large effect on the specific ethanol production rate. The literature (3) and partial evidence presented in Section 3.4 suggested that increased glucose-6-phosphate dehydrogenase activity was responsible for the enhanced fermentation flux.

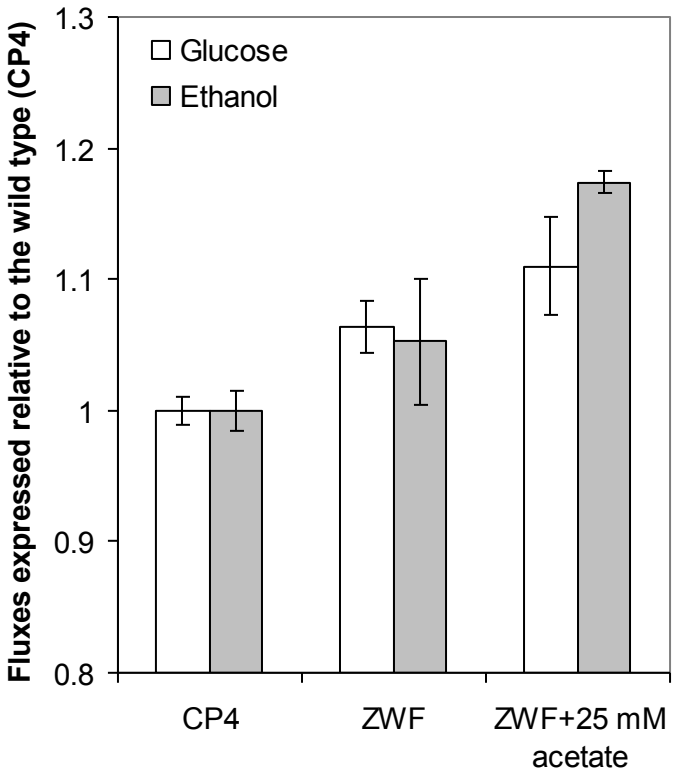

Fig. 3.1 *In vivo* fluxes measured by ^{13}C NMR in non-growing *Z. mobilis* wild type (CP4), the recombinant containing plasmid for over-expressing glucose-6-phosphate dehydrogenase (CP4 + pLOI711 – refer to ZWF in figure), as well as addition of 25 mM acetate to CP4 + pLOI711. Fluxes are expressed relative the wild type, with error bars indicating SEM (*n*=2). The cell density was OD_{550} = 100, with dry weight specifically determined for CP4 (22.13 mg/ml; SEM=0.24 *n*=3) and CP4 + pLOI711 (24 mg/ml; SEM=0.08 *n*=4). The cellular volume (CP4=6.64 % (v/v); CP4 + pLOI711 =7.2 % (v/v)) was estimated by using the conversion factor 3 µl.mg^{-1} dry weight (36). The starting glucose concentration was 100 mM (unlabeled). *In vivo* ^{13}C NMR fluxes were measured with the following pulse parameters: pulse duration (6 µs), flip angle (45^{o}), acquisition time (0.65 s), broadband ^{1}H decoupling (continuous), pre-acquisition time (zero). The rest of the NMR parameters were as in Chapter 5. Peaks were analyzed by deconvolution (line-broadening 10 Hz).

The glucose and ethanol resonances used for determining fluxes in Figure 3.1 were not calibrated for NMR relaxation, which resulted in the fact that glucose and ethanol flux values could not be stoichiometrically compared, and that a quantitative conversion ratio of glucose to ethanol could therefore not be determined (data not shown). Ethanol resonances were not calibrated since we were interested in relative flux changes in response to the modulations. This was also the case for the first 2 supply-demand experiments (Sections 3.2 and 3.3).

3.2) First supply-demand experiment

In order to assess the flux control distribution between glycolytic supply and ATP demand, as well as the contributions to ATP or NTP homeostasis, the elasticities of supply and demand toward the ATP/ADP and NTP/NDP ratios were determined. Investigation of NTP/NDP based elasticities is supported by previous kinetic work with the *Z. mobilis* glucokinase enzyme, which has shown that nucleoside triphosphates (ATP, UTP, GTP, ITP, and CTP) are indiscriminately utilized for glucose phosphorylation (45). Supply elasticities were determined by incubating cells with increasing levels of acetate (to modulate the demand for ATP), followed by glucose addition, and then the separate determination of fermentation fluxes (*in vivo* ^{13}C NMR spectroscopy) and ATP/ADP as well as NTP/NDP ratios (by preparation of cell free extracts for ^{31}P NMR spectroscopy). Demand elasticities were determined similarly, the perturbations in this case being in the ATP supply block by using recombinants over-expressing glucose-6-phosphate dehydrogenase (CP4 + pLOI711) or the glucose facilitator (CP4 + pLOI710 – refer to GLF in figures).

The nucleoside phosphate concentrations, as well as the ATP/ADP and NTP/NDP ratios for the different modulations are shown in Figure 3.2. Demand modulation (acetate) led to decreasing levels of ATP and increasing ADP levels, with decreases observed for the ATP/ADP ratio (compared to the reference state CP4). While UTP levels decreased compared to the reference state, the same gradual decreases observed for ATP were not evident. Furthermore XDP levels increased with increasing acetate levels, with the

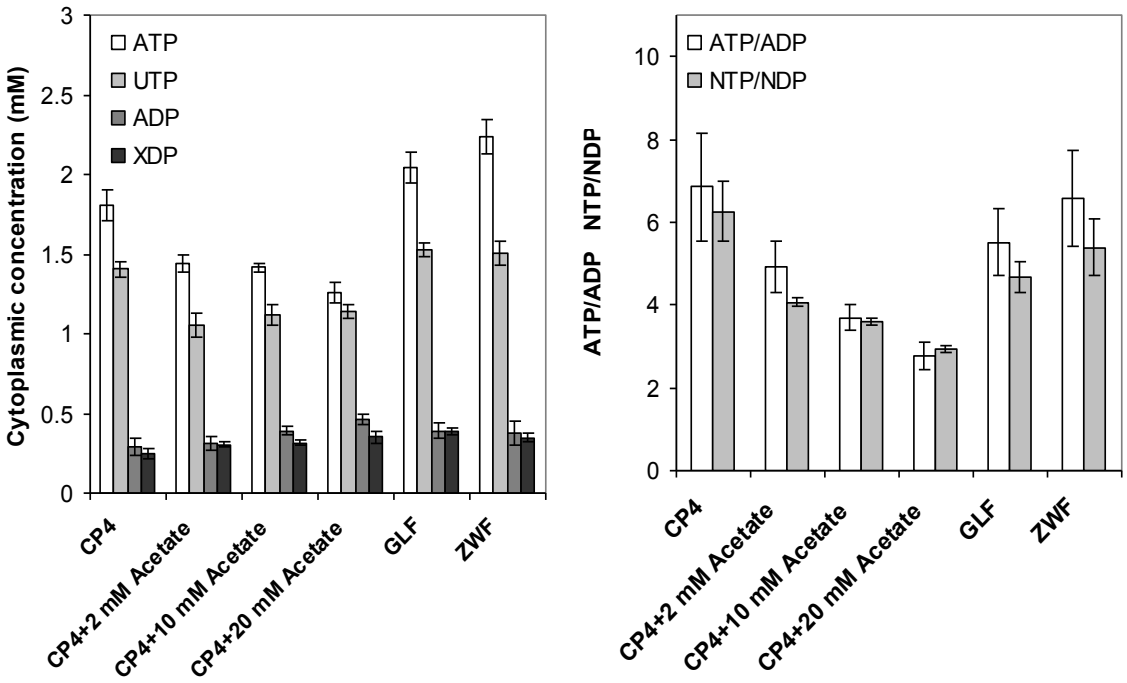

Fig 3.2 Extracts made during the non-growing fermentation of glucose by the wild type *Z. mobilis* (CP4), CP4 with the addition of acetate (2 mM, 10 mM and 20 mM), as well as the recombinants CP4 + pLOI710 (over-expression of the glucose facilitator – refer to GLF in figure) and CP4 + pLOI711 (over-expression of glucose-6-phosphate dehydrogenase – refer to ZWF in figure), were analyzed with ^{31}P NMR spectroscopy. Error bars indicate SEM *n*=4. Dry weight was specifically determined for CP4 (22.8 mg/ml; SEM=0.2 *n*=3), CP4 + pLOI710 (24 mg/ml; SEM=0.22 *n*=4), and CP4 + pLOI711 (23.95 mg/ml; SEM=0.32 *n*=4). The cytoplasmic volume (CP4=5.47 % (v/v), CP4 + pLOI710 (5.76 % (v/v) and CP4 + pLOI711 =5.75 % (v/v)) was estimated by using the conversion factor 2.4 µl.mg^{-1} dry weight (36). The γ -NTP and β -NDP resonances were used for determining ATP/ADP and NTP/NDP ratios. Abbreviation: XDP, unidentified beta-nucleoside di-phosphate. The NMR parameters are described in Chapter 5.

NTP/NDP (ATP+UTP)/(ADP+XDP) ratio decreasing. Over-expression of the glucose facilitator (CP4 + pLOI710, supply modulation) led to increases in ATP, ADP, UTP as well as XDP levels, with the ATP/ADP ratio and the NTP/NDP ratio decreasing. Finally

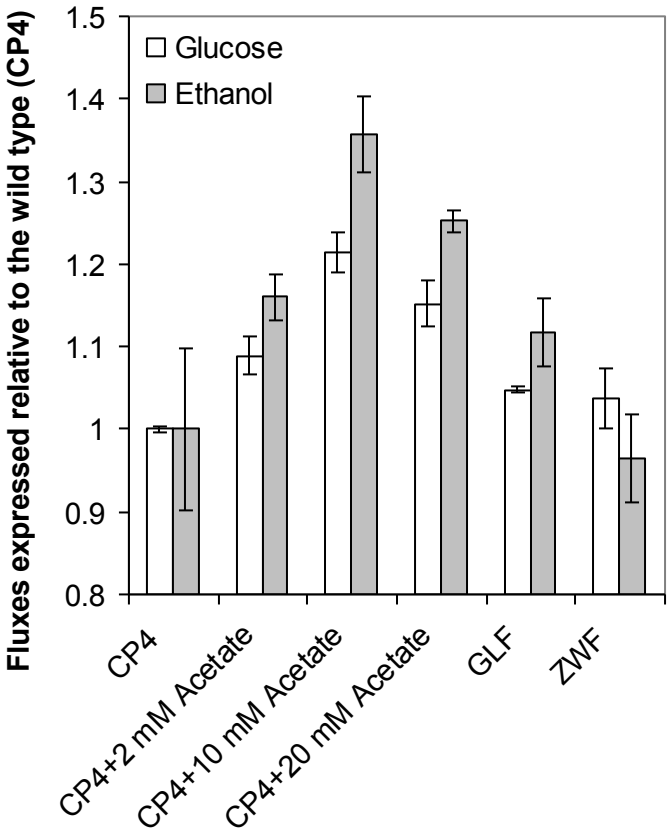

Fig. 3.3 *In vivo* fluxes measured by ^{13}C NMR in non-growing *Z. mobilis* wild type (CP4), CP4 with the addition of acetate (2 mM, 10 mM and 20 mM), as well as the recombinants CP4 + pLOI710 (over-expression of the glucose facilitator – refer to GLF in figure) and CP4 + pLOI711 (over-expression of glucose-6-phosphate dehydrogenase – refer to ZWF in figure). Fluxes are expressed relative to the wild type, with error bars indicating SEM (*n*=2). Dry weight and glucose addition were as described in Figure 3.2. The cellular volume (CP4=6.84 % (v/v), CP4 + pLOI710 7.2 % (v/v) and CP4 + pLOI711 =7.19 % (v/v)) were estimated by using the conversion factor 3 µl.mg^{-1} dry weight (36). *In vivo* ^{13}C NMR fluxes were measured with the following pulse parameters: pulse duration (6 µs), flip angle (45^{o}), acquisition time (0.65 s), broadband ^{1}H decoupling (continuous), pre-acquisition time (zero). The other NMR parameters were as described in Chapter 5. Peaks were analyzed by deconvolution (line-broadening 10 Hz).

over-expression of glucose-6-phosphate dehydrogenase (CP4 + pLOI711) led to increases in ATP, XDP, UTP and ADP, with the corresponding ATP/ADP and NTP/NDP

ratios decreasing. The respective supply and demand flux responses toward the modulated ATP/ADP and NTP/NDP ratios are shown in Figure 3.3. Except for the ethanol flux of CP4 + pLOI711, all fluxes were stimulatory compared to the reference state.

Figure 3.4 shows the sensitivity of the supply flux toward the ATP/ADP ratio and the NTP/NDP ratio (ATP+UTP)/(XDP+ADP). The lines are linear regressions of the data, and indicate the elasticities of supply in terms of glucose and ethanol fluxes. The 20 mM acetate modulation was excluded from the elasticity analysis. It appeared as if the 20 mM acetate was too high, and secondary negative effects were observed. With the acetate modulation experiments we aimed to make small perturbations in the ATP/ADP ratio and analyze the effect on the supply flux. We did not aim at making large perturbations, and

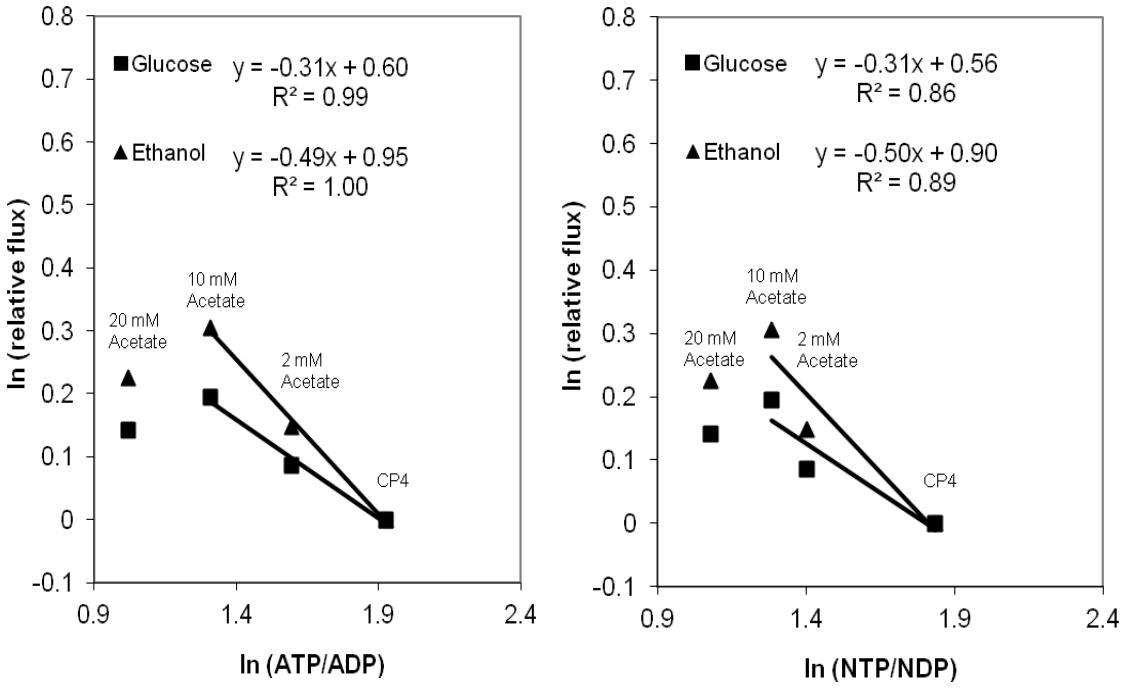

Fig. 3.4 The sensitivity of the supply fluxes toward the ATP/ADP and NTP/NDP ratios. Non-growing fluxes were determined as described in Fig 3.3 and nucleoside phosphates were determined as described in Fig 3.2. The same cultures used for preparing extracts were used for simultaneous *in vivo* flux measurement. Abbreviations: CP4, wild type *Z. mobilis* – acetate were added to CP4.

needed to extrapolate the experimental results back to the non modulated state. For this reason we excluded the 20 mM acetate in this analysis and in further experiments. The 20 mM acetate modulation shows further decreases in both the ATP/ADP and NTP/NDP ratios, with concomitant decreased supply flux. The supply elasticity toward the ATP/ADP ratio was –0.31 for the glucose flux and –0.49 for the ethanol flux. The supply elasticity toward the NTP/NDP ratio was –0.31 for the glucose flux and –0.50 for the ethanol flux.

In Figure 3.5 the sensitivity of the demand (determined as glucose or ethanol fluxes) toward the ATP/ADP ratio and the NTP/NDP ratio (ATP+UTP)/(XDP+ADP) is shown.

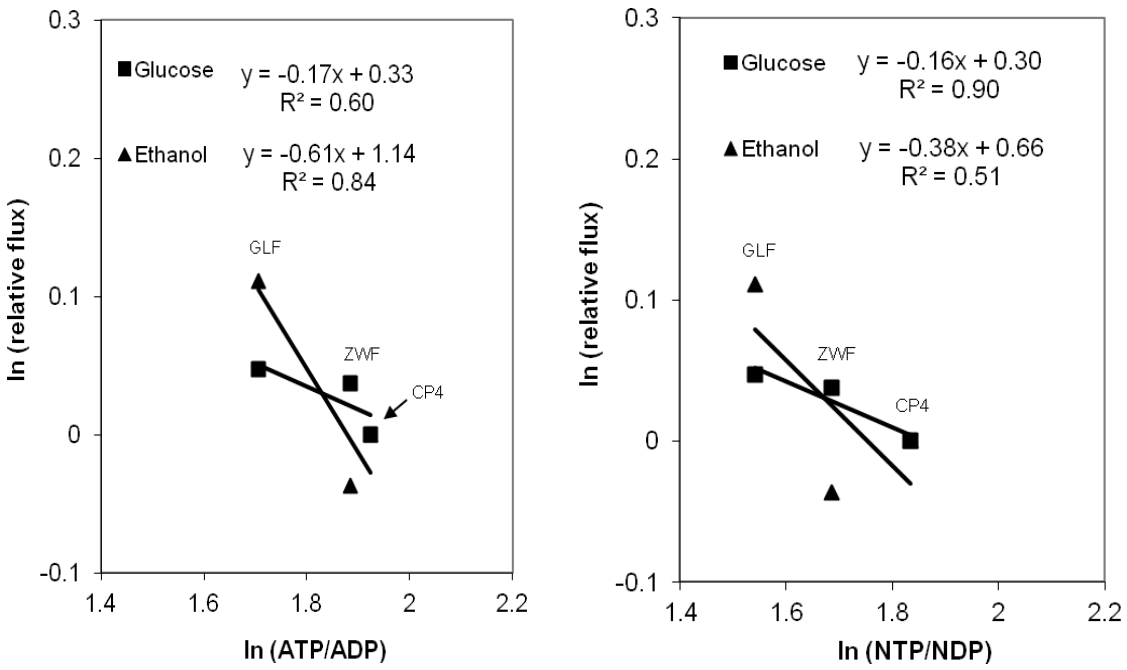

Fig. 3.5 The sensitivity of the demand toward the ATP/ADP and NTP/NDP ratios. **N**on-growing fluxes were determined as described in Fig 3.3 and nucleoside phosphates were determined as described in Fig 3.2. The same cultures used for preparing extracts were used for simultaneous *in vivo* flux measurement. Abbreviations: CP4, wild type *Z. mobilis*; CP4 + pLOI710, over-expression of the glucose facilitator (refer to GLF in figure); CP4 + pLOI711, over-expression of glucose-6-phosphate dehydrogenase (refer to ZWF in figure).

The lines are linear regressions of the data, and indicate the elasticities of demand in terms of glucose and ethanol fluxes. The demand elasticity toward the ATP/ADP ratio was –0.17 for the glucose flux and –0.61 for the ethanol flux. The demand elasticity toward the NTP/NDP ratio was –0.16 for the glucose flux and –0.38 for the ethanol flux.

We do not have sufficient confidence in the absolute values of the elasticities of supply and demand determined here to calculate the values of the flux- and concentration-control coefficients from them; the control coefficient values are therefore not presented. This is discussed further in Chapter 4.

3.3) Second supply-demand experiment

Three modifications were made to the experimental protocol for the second supply-demand experiment. The first modification was aimed at getting more accurate steady-state time courses for the ATP/ADP and NTP/NDP ratios, since a slight drop in anaerobic cellular energy state levels occurred towards the end of the fermentation in the first supply-demand experiment (data not shown), probably due to glucose depletion. The time frame for extractions was therefore shifted from 5–8 min to 3.5–6.5 min. The second modification was motivated by the observation that supply activity was not further increased through addition of 20 mM acetate, prompting reduction of the most extreme demand modulation to 10 mM acetate (Figures 3.3 and 3.4). The third modification, based on the observation that over-expression of flux stimulatory glycolytic enzymes reduced the anaerobic cellular energy state (i.e. the CP4 + pLOI710 and CP4 + pLOI711 supply modulations in Figures 3.3 and 3.5), centred on quantifying the energy demand caused by plasmid maintenance. Our hypothesis was that the energy demand for maintaining plasmids reduced the anaerobic cellular energy sate.

The nucleoside phosphate concentrations, as well as the ATP/ADP and NTP/NDP ratios for the different modulations are shown in Figure 3.6. For the demand modulations (acetate addition) the ATP/ADP ratio decreased slightly compared to the reference state (CP4) for the 2 mM and 10mM acetate modulations, with the ATP/ADP ratio of the

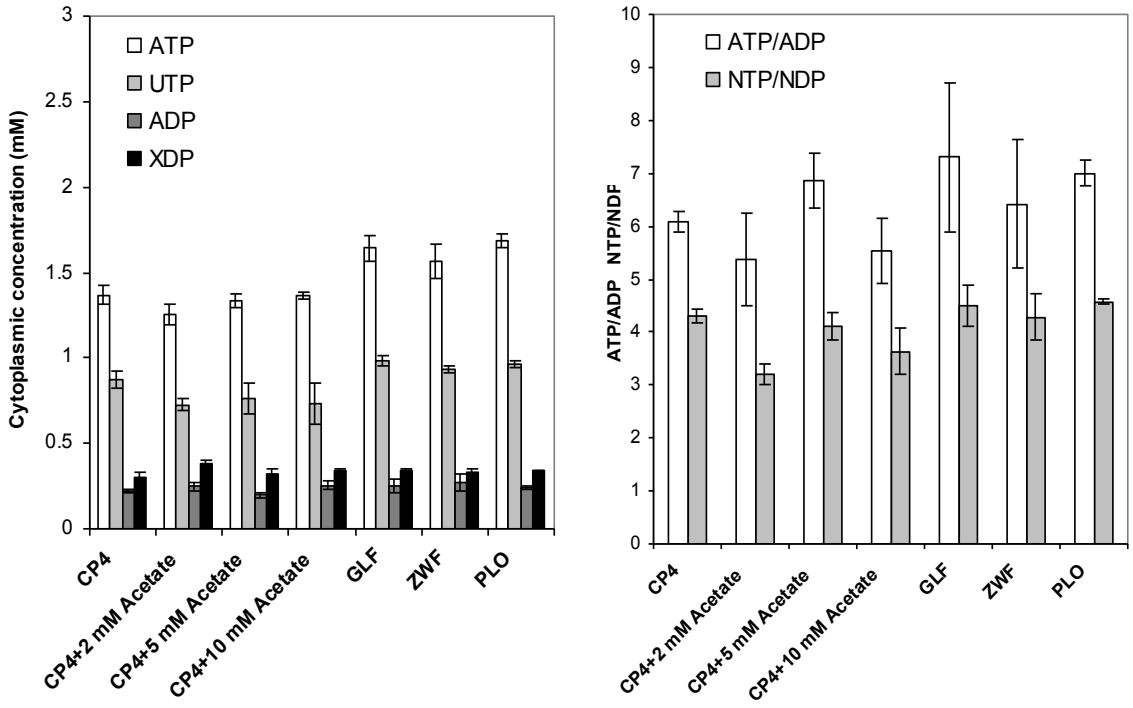

Fig. 3.6 Extracts made during the non-growing fermentation of glucose by the wild type *Z. mobilis* (CP4), CP4 with the addition of acetate (2 mM, 5 mM and 10 mM); as well as the recombinants CP4 + pLOI706EH (non-expressing plasmid – refer to PLO in figure), CP4 + pLOI710 (over-expression of the glucose facilitator – refer to GLF in figure) and CP4 + pLOI711 (over-expression of glucose-6-phosphate dehydrogenase – refer to ZWF in figure); were analyzed with ^{31}P NMR spectroscopy. Error bars indicate SEM *n*=4. Dry weight was specifically determined for CP4 (18.13 mg/ml; SEM=0.41 *n*=3), CP4 + pLOI706EH (22.1 mg/ml; SEM=0.47 *n*=3), CP4 + pLOI710 (20.33 mg/ml; SEM=0.18 *n*=3), and CP4 + pLOI711 (21.47 mg/ml; SEM=0.07 *n*=3). The cytoplasmic volume (CP4=4.35 % (v/v), (CP4 + pLOI706EH =5.3 % (v/v), CP4 + pLOI710 (4.88 % (v/v) and CP4 + pLOI711 =5.15 % (v/v)) was estimated by using the conversion factor 2.4 µl.mg^{-1} dry weight (36). The γ-NTP and β-NDP resonances were used for determining ATP/ADP and NTP/NDP ratios. Abbreviation: XDP, unidentified beta-nucleoside di-phosphate. The NMR parameters are described in Chapter 5.

5 mM acetate modulation increasing slightly. However, all these changes were very small and not significant. The NTP/NDP ratio decreased for all the acetate conditions. In contrast to the first supply-demand experiment, where gradual increases in acetate levels were associated with gradual decreases in both the ATP/ADP and NTP/NDP ratios, this correlation was not observed in the second supply-demand experiment.

The supply modulations did not change the NTP/NDP ratio, with both the CP4 + pLOI710 and CP4 + pLOI711 modulations slightly increasing the ATP/ADP ratio. The ATP/ADP ratio of the recombinant containing a non-expressing plasmid (CP4 + pLOI706EH - refer to PLO in figures) increased compared to the reference state (CP4), with no change observed for the NTP/NDP ratio.

Figure 3.7 shows that flux responses towards both the supply and demand modulations were again stimulatory. The glucose and ethanol flux of the *Z. mobilis* recombinant containing a non-coding plasmid (CP4 + pLOI706EH) was also faster compared to the reference state (wild-type CP4, not containing any plasmid).

Elasticities were not calculated for the second supply-demand experiment as there was no correlation between the cellular free-energy state and the concomitant flux responses for either supply or demand. Control coefficients could therefore also not be determined.

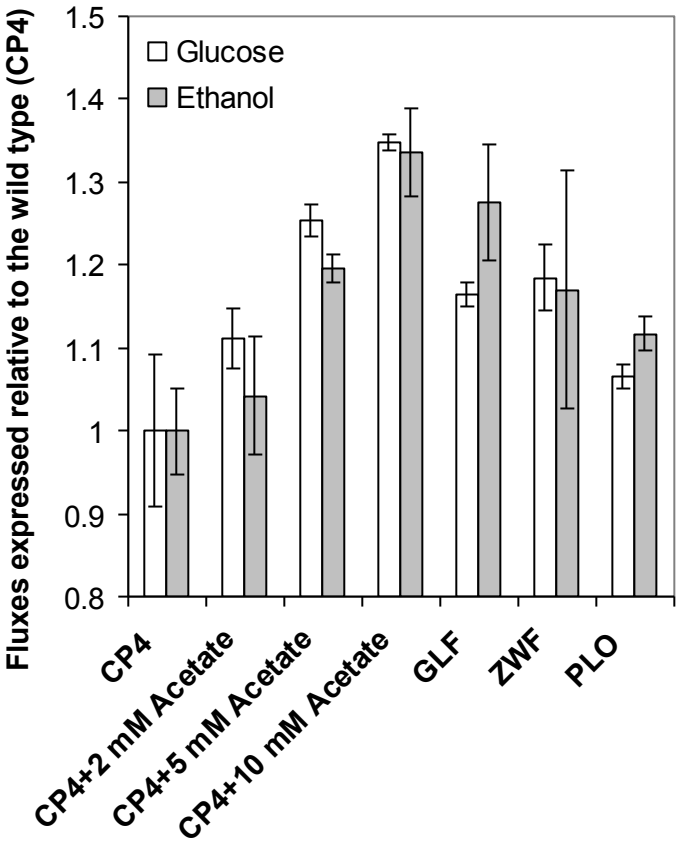

Fig. 3.7 *In vivo* fluxes measured by ^{13}C NMR in non-growing *Z. mobilis* wild type (CP4), CP4 with the addition of acetate (2 mM, 5 mM and 10 mM); as well as the recombinants CP4 + pLOI706EH (non-expressing plasmid – refer to PLO in figure), CP4 + pLOI710 (over-expression of the glucose facilitator – refer to GLF in figure) and CP4 + pLOI711 (over-expression of glucose-6-phosphate dehydrogenase – refer to ZWF in figure). Fluxes are expressed relative to the wild type, with error bars indicating SEM (*n*=2). Dry weight and glucose addition were as described in Figure 3.6. The cellular volume (CP4=5.44 % (v/v), CP4 + pLOI706EH =6.62 % (v/v), CP4 + pLOI710 (6.10 % (v/v) and CP4 + pLOI711 =6.44 % (v/v)) was estimated by using the conversion factor 3 µl.mg^{-1} dry weight (36). *In vivo* ^{13}C NMR fluxes were measured with the following pulse parameters: pulse duration (6 µs), flip angle (45^{o}), acquisition time (0.65 s), broadband ^{1}H decoupling (continuous), pre-acquisition time (zero). The other NMR parameters were as described in Chapter 5. Peaks were analyzed by deconvolution (line-broadening 10 Hz).

3.4) Growth analysis and recombinant enzyme levels

In the supply-demand experiments changes in the supply-modulated ATP/ADP and NTP/NDP ratios were inconsistent. It is therefore not feasible to draw conclusions about the anaerobic free energy levels of the recombinant containing a non-expressing plasmid (CP4 + pLOI706EH), compared to the reference state (CP4) (Figure 3.6). Recall that the CP4 + pLOI706EH recombinant was investigated in the second supply-demand experiment to verify whether the decreased ATP/ADP and NTP/NDP ratios of the supply modulations (CP4 + pLOI710 and CP4 + pLOI711) observed in the first supply-demand experiment were caused by plasmid maintenance. However, the CP4 + pLOI706EH recombinant did not provide evidence of plasmid-dependent energy demand. Therefore, rather than re-measuring the ATP/ADP and NTP/NDP ratio levels of the CP4 + pLOI711, CP4 + pLOI710 and CP4 + pLOI706EH recombinants, alternative means were used to further investigate the physiological responses of recombinants containing plasmids for over-expressing flux stimulatory enzymes. In Table 3.1 it can be seen that all the recombinants (including CP4 + pLOI706EH) grew slower and had lower expression levels of phosphoglycerate kinase and pyruvate kinase compared to the wild type *Z. mobilis* (CP4). As expected, the CP4 + pLOI711 recombinant had clearly elevated glucose-6-phosphate dehydrogenase activity compared to the wild type and other recombinants.

Table 3.1 Specific growth rate (μ) and recombinant enzyme activity. Errors indicate SEM of both the enzyme activity and growth data (n=2 for enzyme activity determinations and for growth determinations n=5 (CP4), n=4(CP4 + pLOI710), n=3(CP4 + pLOI711, CP4 + pLOI706EH)). Abbreviations: G6PDH, glucose-6-phosphate dehydrogenase; PGK, phospoglycerate kinase (EC 2.7.2.3); PK, pyruvate kinase; CP4, *Z. mobilis* wild type strain; CP4 + pLOI706EH , CP4 containing non-expressing plasmid; CP4 + pLOI710, CP4 containing plasmid for overexpressing the glucose facilitator; CP4 + pLOI711, CP4 containing plasmid for overexpressing glucose-6-phosphate dehydrogenase.

Wild type and recombinants	μ (h^{-1})	G6PDH (IU.mg protein^{-1})	PGK (IU.mg protein^{-1})	PK (IU.mg protein^{-1})
CP4	0.515 ± 0.009	0.57 ± 0.07	1.61 ± 0.15	2.34
CP4 + pLOI706EH	0.480 ± 0.001	0.58 ± 0.06	1.30 ± 0.06	2.00
CP4 + pLOI710	0.489 ± 0.008	0.61 ± 0.05	1.35 ± 0.07	2.07
CP4 + pLOI711	0.488 ± 0.014	0.66 ± 0.07	1.34 ± 0.10	2.06

3.5) Third supply-demand experiment

It is clear from Section 3.4 that incorporation of a non-expressing plasmid (CP4 + pLOI706EH) or expressing plasmids (CP4 + pLOI710, CP4 + pLOI711) decreased *Z. mobilis* growth rate as well as the expression of other glycolytic enzymes. Our results showed that these effects were relatively similar for all three recombinants (Table 3.1). We therefore decided to use CP4 + pLOI706EH as the new reference state for the third supply-demand experiment to account for the effects of plasmid transformation. Furthermore a quantitative approach, as discussed in Section 2.2.1.2, was used for *in vivo* ^{13}C NMR flux analysis. This centred on determining an ethanol calibration factor, which was used to scale saturated ethanol resonance and enabled us to determine absolute

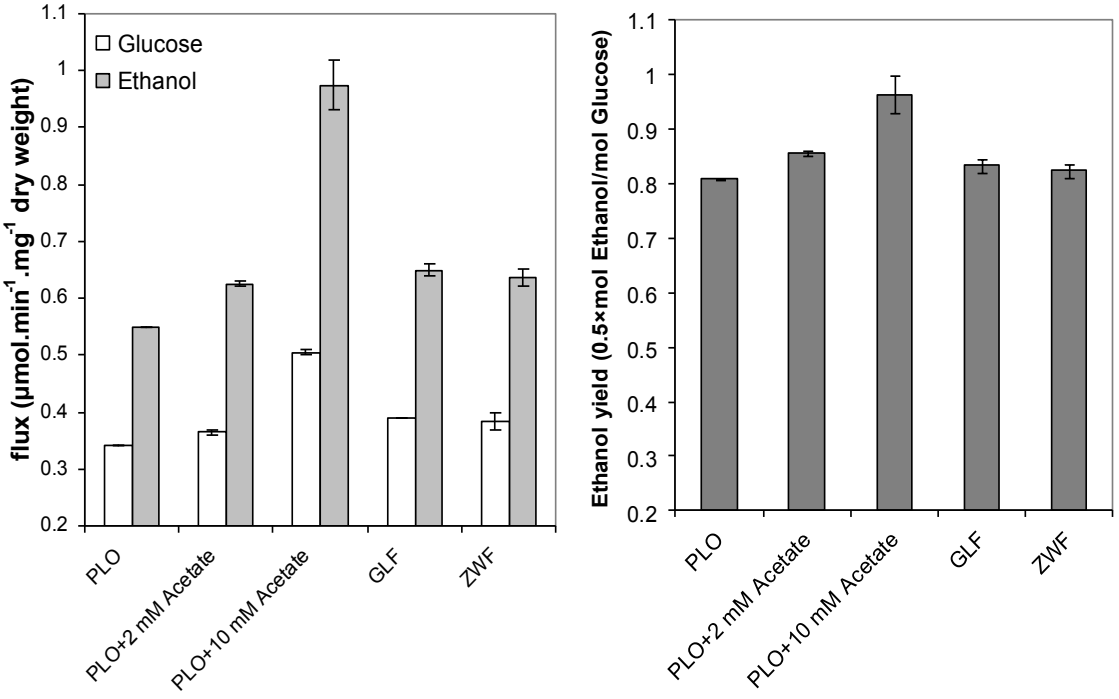

Fig. 3.8 *In vivo* glucose and ethanol fluxes and ethanol yield measured by ^{13}C NMR in non-growing *Z. mobilis* containing a non-expressing plasmid (CP4 + pLOI706EH – refer to PLO in figure), CP4 + pLOI706EH with the addition of acetate (2 mM and 10 mM); as well as CP4 + pLOI710 (over-expression of the glucose facilitator – refer to GLF in figure) and CP4 + pLOI711 (over-expression of glucose-6-phosphate dehydrogenase – refer to ZWF in figure). Fluxes were determined as described in Section 2.2.1.2, with the ethanol saturation factor determined in that experiment used for scaling ethanol resonances. The cell density was OD_{550} = 75, with dry weight specifically determined for CP4 + pLOI706EH (14.49 mg/ml; SEM=0.08 *n*=3), CP4 + pLOI710 (14.64 mg/ml; SEM=0.12 *n*=3), and CP4 + pLOI711 (14.67 mg/ml; SEM=0.10 *n*=3). The cellular volume (CP4 + pLOI706EH =4.35 % (v/v), CP4 + pLOI710 (4.39 % (v/v) and CP4 + pLOI711 =4.4 % (v/v)) was estimated by using the conversion factor 3 µl.mg^{-1} dry weight (36). The starting glucose concentration was 75.73 mM (of which 8.43 mM was [1, 6-$^{13}C_2$]). *In vivo* ^{13}C NMR fluxes were measured with the following pulse parameters: pulse duration (12 µs), flip angle (90^{o}), acquisition time (0.65 s), broadband ^{1}H decoupling (0.65 s during acquisition time), pre-acquisition time (0.35 s). Peaks were analyzed by integration (line-broadening 2 Hz). The other NMR parameters were as presented in Chapter 5.

glucose and ethanol fluxes. The results also allowed us to determine an accurate stoichiometric conversion factor for glucose to ethanol.

Figure 3.8 shows the respective glucose and ethanol flux responses toward the supply and demand modulations, with all fluxes showing increased productivity compared to the CP4 + pLOI706EH reference state. Glucose fluxes were estimated in a similar manner as in Section 2.2.1.2, with the glucose level at the start of steady-state fermentation determined by using the stoichiometry obtained in that experiment (88 % conversion of carbons 3and 6 of glucose to the methyl group of ethanol). This was in good agreement with an *in vivo* ^{13}C NMR spectrum collected after glucose depletion for CP4 + pLOI706EH +10 mM acetate during this experiment (Figure 3.9).

Unfortunately nucleoside phosphate analysis was unsuccessful in the third supply-demand experiment. This will be further discussed in Chapter 4.

This chapter has presented results of three experiments investigating the effect of perturbations in the cellular energy state on glycolytic flux and nucleotide ratios. The effect of transforming the *Z. mobilis* strain with various plasmids on the growth rate and expression levels of certain glycolytic enzymes was also determined. The next chapter discusses these results and places them in the broader context of existing scientific literature.

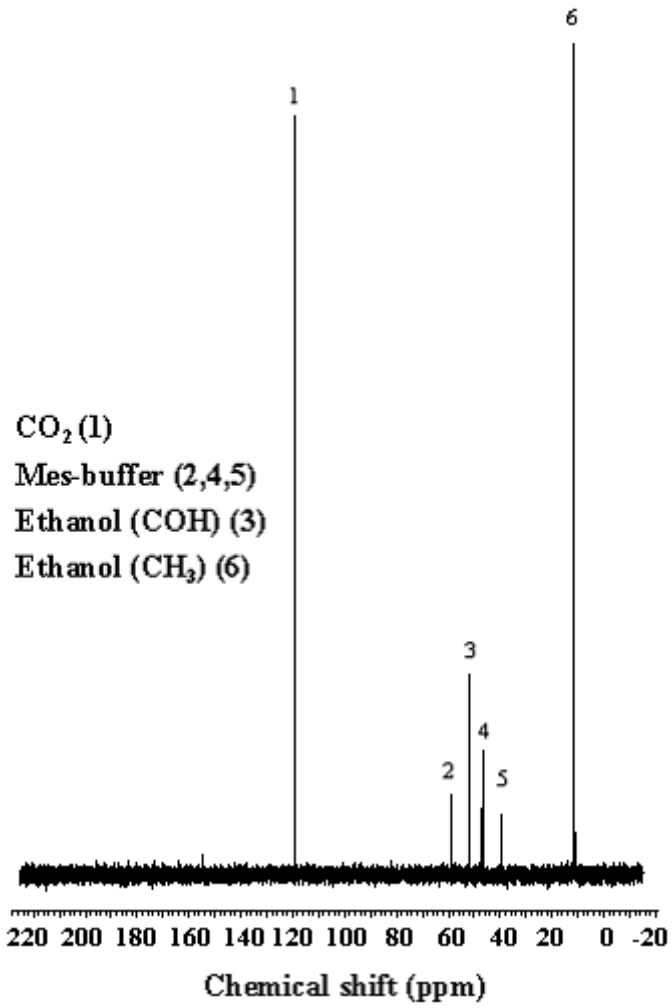

Fig. 3.9 *In vivo* ^{13}C NMR spectrum collected after glucose depletion (CP4 + pLOI706EH + 10 mM acetate). The starting glucose concentration was 75.73 mM (of which 8.43 mM was [1, 6-$^{13}C_2$]). The ethanol yield from glucose can be calculated directly; respectively yielding 88.5 % and 89 % conversion to the hydroxyl and methyl carbons of ethanol. The following pulse parameters was used: pulse duration (12 µs), flip angle (90^o), acquisition time (0.65 s), broadband ^1H decoupling (0.65 s during acquisition time), pre-acquisition time (15 s), transients (+/- 48). Other NMR parameters were as in Chapter 5.

Chapter 4

General discussion

4.1) Synopsis

This thesis has described the investigation of the regulation of anaerobic free-energy metabolism in *Z. mobilis* with an experimental approach. The key features of our experimental setup were the use of NMR spectroscopy for detecting metabolites, as well as employing non-growing conditions for supply-demand experiments. *In vivo* ^{13}C NMR spectroscopy was used for measuring fluxes, while nucleotide levels were analysed in cell-free extracts due to difficulty with detecting *in vivo* NDP with ^{31}P NMR. The use of non-growing conditions simplified the analysis by enabling us to correlate glycolytic flux stoichiometrically with the ATP production rate.

Fermentation of glucose was investigated in the wild type *Z. mobilis* (CP4), a recombinant containing a non-expressing plasmid (CP4 + pLOI706EH), or expressing plasmids for over-expressing the glucose facilitator (CP4 + pLOI710) or glucose-6-phosphate dehydrogenase (CP4 + pLOI711). In addition, ATP demand in the non-expressing recombinant and wild type were perturbed by titrating with the uncoupler acetic acid. Our results show that the anaerobic free-energy demand, the glucose facilitator and glucose-6-phospate dehydrogenase all control the flux of ethanol production in *Z. mobilis*. The Entner-Doudoroff glycolytic supply activity was found to be sensitive to changes in the ratios of ATP/ADP (elasticity varied between –0.31 and –0.49) and NTP/NDP (elasticity was between –0.31and –0.50).

4.2) Critique

In this section we critically evaluate our data in the context of existing work and the scientific literature. The discussion is structured to cover the glycolytic free-energy supply, the demand for free energy, and measurement of intracellular nucleotide levels.

4.2.1) The supply

Supply elasticities obtained in the first supply-demand experiment had good linear fits. Recall that the values of the supply elasticities towards ATP/ADP were –0.31 (R^2=0.99) using glucose-based flux values and –0.49 (R^2=0.99) for ethanol-based flux values. In the second and third supply-demand experiments, the supply flux again increased in response to acetate titration (Figures 3.7 and 3.8). There was, however, no correlation between the ATP/ADP ratio (and NTP/NDP ratio) and glycolytic flux during the second supply-demand experiment, as was observed for the first experiment. Nucleotide data for the third experiment are not reported, as their spectrophotometric assay was unsuccessful (discussed further below).

This thesis forms part of a project in our laboratory to compare glycolytic regulation in different micro-organisms (i.e. *Z. mobilis*, *E. coli, S. cerevisiae* and *L. lactis*). These organisms were chosen based on their usage of different glycolytic mechanisms, as well as the large volume of information already available in the literature regarding their fermentative physiology. By using similar conditions (non-growing), we ask the question whether mechanistically distinct free energy supplies fulfil the same (or different) regulatory functions in terms of flux control over free-energy production and free-energy homeostasis. We are now in a position to compare supply elasticities obtained for the Entner-Doudoroff glycolytic pathway (*Z. mobilis*) with organisms that utilize the Embden-Meyerhof-Parnas (EMP) glycolytic pathway. Both *S. cerevisiae* and *E. coli* utilize the EMP glycolytic pathway, and in previous ATP/ADP based supply-demand experiments supply elasticity values of –0.84 and –0.89 were respectively obtained (44, 31). Our values are approximately half of those which were found for *S. cerevisiae* and *E. coli*. They are, however, in the same range and point to similar quantitative responses of the glycolytic pathway to changes in ATP/ADP levels amongst the three organisms.

Since the *Z. mobilis* supply has a negative elasticity value, the Entner-Doudoroff glycolytic pathway should be mechanistically equipped to be regulated by ATP or ADP, as is the case with the Embden-Meyerhoff-Parnas glycolytic pathway (i.e. *via*

phosphofructokinase). Since both pathways have the same enzyme content in the lower ATP-generating phase of glycolysis, and glucokinase is present in the energy investment phase of the Entner-Doudoroff pathway, both pathways have constituent enzymes interacting with ATP and ADP (i.e. kinase enzymes, see Figure 1.1). There is, however, to our knowledge no evidence in the literature suggesting that any Entner-Doudoroff glycolytic enzyme responds in an allosteric or cooperative manner towards ATP or ADP. Whether cooperative or allosteric type enzymatic interactions with ATP or ADP are a prerequisite for the responses seen for the supply towards varying ATP/ADP ratios, is beyond the scope of this thesis (the possible relevance of allosteric enzymes with regard to glycolytic flux control lies in their ability to respond more sensitively to changes in the levels of energy metabolites than enzymes with Michaelian kinetics; they are expected therefore to better mediate glycolytic responses in order to satisfy overall cellular free-energy needs). It should be noted, though, that cooperativity is not required to explain our data, since the absolute values of the elasticities are less than one.

Previous kinetic work with the *Z. mobilis* glucokinase enzyme has shown that nucleoside phosphates (ATP, UTP, GTP, ITP, and CTP) are indiscriminately utilized for glucose phosphorylation (45). Other workers have also found that UTP, as measured from cell free extracts with ^{31}P NMR spectroscopy, occurs at levels comparable to ATP in *Z. mobilis* (13). It might therefore be possible that the Entner-Doudoroff pathway is regulated by nucleoside phosphates other than adenylates. In our own data, NTP/NDP based supply elasticities of –0.31 and –0.50 were obtained for glucose and ethanol fluxes, respectively (Figure 3.4). These values are virtually identical to the ATP/ADP elasticities, and therefore support this idea.

4.2.2) The demand

The finding by Snoep *et. al.* that glucose-6-phosphate dehydrogenase and the glucose facilitator have flux control over *Z. mobilis* fermentative ethanol production (3), led us to use these enzymes for modulating the supply. Under growing conditions glucose-6-phosphate dehydrogenase has a flux control coefficient of 0.4 over ethanol production

(3); this result has been supported by data suggesting that glucose-6-phosphate levels are saturating for this enzyme (13). Our results support these findings, with enzyme analysis showing increased glucose-6-phosphate dehydrogenase activity (Table 3.1), as well as enhanced fermentative flux for the recombinant over-expressing glucose-6-phosphate dehydrogenase (Sections 2.2.1.1, 3.1-3.3 and 3.5). Our results are therefore also in agreement with work performed under growing conditions, which indicate that the glucose facilitator has partial flux control over ethanol production (3).

The finding that the various recombinants in our study have increased fermentative productivity, but decreased specific growth rate, lends weight to the theory that *Z. mobilis* growth is uncoupled from energy production (Table 3.1, Section 3.4). As proposed by Kalnenieks (20), the membrane F_0F_1-type H^+-ATPase might be the key to understanding *Z. mobilis* uncoupled growth. The energy-dependent futile cycling of protons recycles ADP, a prerequisite for maintaining the rapid catabolic flux observed for *Z. moblis.* It has furthermore been proposed that this rapid catabolic flux is an evolutionary protection mechanism (3). The rapid and massive production of ethanol gives *Z. mobilis* an edge over its competitors, since *Z. mobilis* is highly ethanol resistant (24). It is further discussed that this phenomenon emerges from the insufficient energy yield ($Y_{ATP/Glucose}$=1) of the Entner-Doudoroff pathway, the recycling of ADP by the F_0F_1-type H^+-ATPase, as well as the absence of regulatory enzymes in the 6-carbon intermediate part of glycolysis. Therefore, both above-mentioned studies mention the possible importance of the F_0F_1-type H^+-ATPase in maintaining the rapid catabolic flux observed for *Z. mobilis*.

We also investigated the sensitivity of the non-growing energy demand towards the ATP/ADP and NTP/NDP ratios. While we did not know the exact identity of the no-growing energy demand, the F_0F_1-type H^+-ATPase is proposed to be a substantial contributor (26, 27). For the first supply-demand experiment the data seem to indicate that both supply and demand have negative elasticity values, since both reaction blocks were stimulated by ATP/ADP and NTP/NDP ratios lower than the reference state (Figure 3.5). Therefore, both the supply and demand tended to increase the level of the

linking metabolite when perturbed, and put simply, both blocks appear to act as energy supplies. Is such a scenario possible? As discussed above, fermentation acts as the natural free-energy supply. It could also be possible for the energy demand, which under the non-growing conditions employed by us included the membrane bound F_0F_1-type H^+-ATPase, to act as aerobic energy supply through respiration and oxidative phosphorylation (23). However, we disregard this possibility because fermentation product analysis showed that, within experimental error, under our conditions *Z. mobilis* free-energy generation was proceeding anaerobically through fermentation for the reference and all modulated states (Figure 2.3). This makes it highly unlikely that the F_0F_1-type H^+-ATPase was operating in an ATP-synthesis mode. Furthermore, the demand elasticity values obtained for glucose fluxes (–0.17 w.r.t. ATP/ADP; –0.16 w.r.t. NTP/NDP) and ethanol fluxes (–0.61 w.r.t. ATP/ADP; –0.38 w.r.t NTP/NDP) were not in good agreement; with the linear fits also not very good. While demand elasticities were negative in the first supply-demand experiment, slight increases in ATP/ADP and NTP/NDP ratios were observed in the second supply-demand experiment (accompanied by stimulatory flux responses – and therefore positive elasticities; rate characteristics not shown, refer to Figures 3.6 and 3.7).

The hypothesis at the outset of this thesis was that anaerobic free energy is a significant regulator of the Entner-Doudoroff glycolytic pathway. We set out to answer this question quantitatively, but ultimately struggled to obtain demand elasticities, making it impossible to arrive at a quantitative answer (i.e. flux control, free energy homeostasis in terms of concentration control on ATP/ADP, or both).

4.2.3) Nucleoside phosphate determinations

The finding by biotechnologists that acetate de-energizes *Z. mobilis,* probably through acidification of the cytoplasm (42), led us to use acetate as modulator for increasing the cellular free-energy demand. It has been found that the de-energizing effect of acetate leads to enhanced fermentative productivity, with maximal energetic uncoupling in hydrolysate fermentation media obtained at 30 mM acetic acid (pH 5, Ref. 42). Other work with *Z. mobilis* found that acetate lowers NTP levels in a batch type *in vivo* ^{31}P

NMR setup, and was unable to show the effect of acetate on NDP levels as they were below the limit of detection (46). It should furthermore be kept in mind, as proposed in Chapter 2, that it is the protonated form of acetic acid that mediates energetic uncoupling. In our own results for the first supply-demand experiment 20 mM acetate, which corresponds to 7 mM of the protonated form of acetic acid at pH 5, led to maximal energetic uncoupling (Figure 3.2).

^{31}P NMR spectroscopy has previously been used to measure nucleoside phosphates in *Z. mobilis* by Barrow *et. al*. (13) who also used extracts prepared during non-growing fermentations, with one of the findings being UTP levels that exceed ATP levels (which is in agreement with the high UTP levels we measured). They determined the ATP/ADP ratio (2.8) and the NTP/NDP (ATP+UTP/UDP+ADP) ratio (3.9), with reported errors of 20 % on the ^{31}P NMR data (both the ratios are lower than our values). The ATP and ADP level were 1.40 µg.mg^{-1} dry weight and 0.50 µg.mg^{-1} dry weight respectively; compared to 2.2 µg.mg^{-1} dry weight (ATP) and 0.30 µg.mg^{-1} dry weight (ADP) determined for CP4 (the wild type) in this study. De Graaf *et. al.* (14) used *in vivo* ^{31}P NMR spectroscopy to determine cytoplasmic NTP and NDP levels, which respectively yielded 1.9 mM and 0.2 mM, corresponding to a NTP/NDP ratio of 9.5 (which is slightly higher than the NTP/NDP ratio of ~6.5 we determined).

In the third supply-demand experiment problems were encountered with enzymatic ATP and ADP determinations. The technique centres on using coupled enzyme assays, for example ADP was measured with pyruvate kinase and lactate dehydrogenase. The consumption of ADP is stoichiometrically coupled to the consumption of NADH by lactate dehydrogenase, with the decrease in NADH detected at 340 nm with a spectrophotometer. While detection of standards (40 µM – 150 µM) were not problematic, inconsistencies with acquiring a reference or blank reaction made detection difficult during analysis of samples. We tried to solve the problem by assaying ATP and ADP without a reference absorption value. Our strategy was to delay the rapid conversion of substrates to products (reaction has large K_{eq}) by decreasing enzyme levels; and ultimately minimizing detection losses due to the time it takes to place the micro-plate in

the spectrophotometer. The consequence was reaction curves that had a time-span of 45 min to 2 h, and were representative of a multitude of possible contributors. The possible contributors in the case of enzymatic ADP determinations: ADP, XDP (as detected with ^{31}P NMR, Figure 2.7), UDP (13), NADH oxidases (47)). The NADH oxidases are enzymes catalyzing NADH oxidation, and can become especially problematic under circumstances where reactions proceed for a long period (reactions should reach completion in less than 10 min (47)).

4.3) Future Perspectives

While NMR spectroscopy is a relatively insensitive technique, it can lead to the detection of unsuspected metabolites which were not pre-selected for analysis. The detection of free-energy metabolites other than ATP and ADP led us to construct NTP/NDP based supply rate characteristics and calculate the corresponding elasticities, which surprisingly had similar values than those for ATP/ADP. Future investigations can therefore focus on whether enzymes in the energy generation phase of the Entner-Doudoroff glycolytic pathway can for instance utilize UDP/UTP as substrates or products. Furthermore, by again focusing on a top-down approach (30), it would be interesting to compare supply-demand behaviour of the different nucleoside phosphate moieties. This could be done with a similar approach as in this project, with only a few changes to the NMR protocol to enhance the UDP, AMP, and UMP signals (this might be overcome by simply using slightly higher cell densities (i.e. OD_{550} = 150 opposed to OD_{550} = 100 – this will also probably require addition of antifoam since OD_{550} = 100 was close to the foaming threshold). Further modifications might centre on the centrifugation of extracts, i.e. 30 min, 0 ^{0}C, 4332 × g was used for protein and cellular debris sedimentation, which might have been too low a centrifugal force for protein sedimentation, and therefore caused the broadening of signals in the AMP and UMP NMR spectral area (spectra not shown). Lastly, due to time-constraints only 3 h were used for accumulating ^{31}P data, which could especially affect the integration values of NDP (since their signals are lower than NTP signals and therefore more susceptible to signal to noise discrepancies, see Figure 2.7).

To improve the signal to noise ratio longer accumulation times can be used (e.g. 6 h opposed to 3 h).

While the ^{13}C NMR pulse parameters used during the first 2 supply-demand experiments are not compatible with those used during the third supply-demand experiment, results were in good agreement. The fluxes measured during the third supply-demand experiment showed increased accuracy; as gauged by the error bars (compare Figures 3.3, 3.7 and 3.8). It might be argued that the gated ^{1}H decoupling, the introduction of a short recycle delay, or the quantification strategy (i.e., determination of absolute quantities) caused the enhanced accuracy. Our approach, based on analyzing small ADP, XDP, or saturated unlabeled ethanol resonances (which are quite sensitive to experimental noise in the NMR spectra) centres on the increased signal-to-noise ratio attained by using labelled glucose during the third supply-demand experiment. The value of determining absolute quantities in calibrated NMR experiments is, however, clear from the fluxes determined in the third supply-demand experiment. For example, the ethanol stoichiometric yield from glucose fermentation can be inferred. Further advantages of quantitative ^{13}C NMR flux analysis is comparison with previous and future work, as well as providing data that can be incorporated into computer models of *Z. mobilis* fermentation (48).

Our initial aim was to do supply-demand experiments *in vivo*, and as discussed in Chapter 2, *in vivo* resolution of NTP and NDP proved difficult to attain. This could perhaps be solved by using a flow-through type NMR experimental setup, which has been successfully applied to study *Z. mobilis* (14). The question that follows is whether NTP/NDP based elasticities obtained from cell free extracts would differ from *in vivo* NTP/NDP based elasticities. It is certainly an interesting and non-trivial issue since the *in vivo* free NTP/NDP ratio could differ from the total free NTP/NDP ratio (as measured from cell free extracts) due to binding/sequestration of nucleotides by enzymes *in vivo*. Approximately half of the total soluble protein of Z. mobilis is vested in the glycolytic and fermentative enzymes alone (2).

While the focus of the above mentioned work is experimental, theoretical work done in our lab has shown that for different erythrocyte glycolytic models the demand for ATP controls the flux through glycolysis (the demand has low elasticity values toward ATP). Furthermore the supply (i.e. glycolysis) responds sensitively to changes in the level of ATP for the different models (the supply has large negative elasticity values toward ATP). Analysis of different erythrocyte glycolytic models with supply-demand analysis therefore shows that when the energy demand controls the flux through anaerobic free energy metabolism, the supply (i.e. glycolysis) controls the magnitude of the variation of ATP (9, 49).

4.4) Conclusion

The take home message of this thesis is that the anaerobic free-energy demand, the glucose facilitator and glucose-6-phospate dehydrogenase all have a degree of flux control over ethanol production in *Z. mobilis*. Furthermore the supply elasticities show quantitatively that Entner-Doudoroff glycolytic activity is sensitive to changes in ratios of ATP/ADP and NTP/NDP. However, *in vivo* detection of phosphorylated NTP and NDP with NMR spectroscopy was problematic. Finally, the supply elasticities might be useful for future modeling explorations, as was done for erythrocyte glycolysis (49).

Chapter 5

Experimental procedures

5.1) *Z. mobilis* culturing methods and growth analysis

5.1.1) Bacterial strain and plasmids

The *Z. mobilis* wild type and recombinants (Table 5.1) were grown overnight and added to 40 % (V/V) sterile glycerol for storage at –80 ^{o}C. To ensure that recombinants retain the plasmids the antibiotic tetracycline (12.5 µg/mL) was added during all growth experiments (agar plates, overnight, and pre-cultures). Tetracycline was prepared by dissolving in 50 % (V/V) water/ethanol and filter sterilization. Distilled water was used for all experiments where cultures were alive (i.e., plates, growth and non-growing cultures), and de-ionized water was used for all experiments where cultures were dead (i.e., PCA used for extraction, extracted metabolite analysis with ^{31}P NMR, and enzyme assays).

Table 5.1 *Z. mobilis* wild type and recombinants

Wild type and recombinants	Description	Reference
CP4	Wild type	
CP4+pLOI706EH	Non-expressing recombinant	38
CP4+pLOI710	Recombinant over-expressing the glucose facilitator	3
CP4+pLOI711	Recombinant over-expressing glucose-6-phosphate dehydrogenase	3

5.1.2) Growth on agar plates

A small swipe of the *Z. mobilis* freezer stocks was used for growth on agar plates (approximately 50 – 60 h, 30 ^{o}C). For each experiment new plates were prepared. The growth media for agar plates contained the following ingredients per 1 L: 1 g $(NH_4)_2SO_4$, 1 g KH_2PO_4, 0.5 g $MgSO_4.7H_2O$, 10 g yeast extract, 20 g glucose, 15 g agar.

5.1.3) Growth in liquid media

Shake flasks filled to capacity were used for all experiments, with the nozzles of the shake flasks covered with cotton wool and aluminium foil (shaking speed 125 rpm, 30 ^{o}C). Overnight cultures were grown to approximately OD_{550} = 0.2–1, and pre-cultures were grown to OD_{550} = 4 (approximate mid-exponential growth phase). The liquid growth media contained the following ingredients per 1 L: 1 g $(NH_4)_2SO_4$, 1 g KH_2PO_4, 0.5 g $MgSO_4.7H_2O$, 10 g yeast extract, 100 g glucose.

For analyzing the specific growth rates pre-cultures were inoculated at an optical density of approximately OD_{550} = 0.05. Sampling (OD_{550}) was done approximately every hour.

5.2) Metabolite analysis in non-growing cells

Cultures were harvested in mid-exponential phase (OD_{550} = 4) through centrifugation (3580 × g, 20^{o}C, 10 min), and washed once with buffer without a carbon source (100 mM MES, 0.1 % KH_2PO_4, 0.1 % $MgCl_2.6H_2O$ (pH 5)). The washed cultures were concentrated approximately 75-fold to OD_{550} = 300 by re-suspending in a small volume of the wash buffer, and kept at room temperature for analysis.

5.2.1) *In vivo* real time flux and metabolite determinations

5.2.1.1) ^{13}C NMR flux measurement

Ten millimeter NMR tubes with a working volume of 3 ml contained the following components for *in vivo* ^{13}C NMR flux measurement: 2.3 ml cells at final OD_{550} = 75 or OD_{550} = 100 (approximately 15 mg/mL or 20 mg/mL dry weight) suspended in wash buffer (69-73 mM MES (pH 5), 0.069-0.073 % (w/v) KH_2PO_4, 0.069-0.073 % (w/v) $MgCl_2.6H_2O$); 300 µl D_2O (NMR solvent); 200 µl glucose (final concentration 75 mM or 100 mM; labeled glucose [1,6-$^{13}C_2$] fraction sometimes included); and 200 µl distilled water. The 200 µl distilled water space was used for the incremental addition of acetate (pH 5) for the demand modulations. The concentration ranges of the MES-buffer and salts were a consequence of slight variation in the cellular volumes, and therefore the occupation of variable space in the fermentations. The MES-buffer is not transported into the cytoplasm (36). Cellular volumes were estimated by using the conversion factor 3 µl/mg dry weight (36).

Fermentations were done in the following manner: All the components for flux measurement, apart from the glucose were added to the NMR tube and placed in the NMR spectrometer for temperature equilibration and acquiring base-line spectra (10 min, 30 ^{o}C, and 15 Hz sample spin). After glucose addition and light mixing the sample was placed back in the spectrometer and shimmed. Data acquisition commenced 2-3 min after glucose was added (this time-lapse was kept constant in a specific experiment). *In vivo* ^{13}C NMR fluxes were measured on a Varian 600 MHz spectrometer with the following pulse parameters: pulse duration (6 µs or 12 µs), flip angle (45^{o} or 90^{o}), acquisition time (0.65 s), broadband ^{1}H decoupling (continuous or 0.65 s during acquisition time), pre-acquisition time (zero or 0.35 s), transients (96), spectral width (40 000 Hz), frequency (150.88 MHz). Peaks were analyzed by deconvolotion (line-broadening 10 Hz) or integration (line-broadening 2 Hz). Peak area determination as well as the line-broadening was kept constant for specific experiments.

The following calibration strategy was used to quantitatively determine ethanol levels. After all the glucose was consumed ethanol and MES-buffer resonances were analyzed with 2 sets of pulse parameters in intermittent fashion. The first parameter set was as follows: pulse duration (12 μs), flip angle (90^{o}), acquisition time (0.65 s), pre-acquisition time (0.35 s) broadband ^{1}H decoupling (0.65 s during acquisition time), transients (96), spectral width (40 000 Hz), frequency (150.88 MHz). The second parameter set was similar to the first except for the pre-acquisition time (15 s). A calibration factor could now be determined by comparing the ethanol peak intensities of the rapidly pulsed experiment (similar to the pulse parameters used during fermentations) with the ethanol peak intensities of the relaxed experiment. Peaks were analyzed by integration (line-broadening 2 Hz) and the MES-buffer resonances were used as internal standard.

5.2.1.2) ^{31}P NMR measurement of NTP and NDP

The *in vivo* ^{31}P NMR experiment presented in this thesis (Figure 2.6) was done at a cell density of OD_{550} = 400 (approximately 80 mg/mL dry weight), with the operating temperature 30 ^{o}C and the final glucose concentration 250 mM (unlabeled). The experiment was done on a 600 MHz Varian NMR spectrometer, with the following parameters used: pulse duration (10 μs), flip angle (60^{o}), acquisition time (0.34 s), broadband ^{1}H decoupling (continuous), pre-acquisition time (zero), transients (180), spectral width (12 136 Hz), frequency (242 MHz), sample spin (15 Hz).

5.2.2) Cell free detection of metabolites

5.2.2.1) Determination of glucose, ethanol, acetate and glycerol with HPLC

Fermentations were conducted in a similar manner as the *in vivo* flux determinations, except that 15 mL centrifuge tubes were used instead of NMR tubes, and unlabelled glucose was used as substrate.

A water bath (30 ^{o}C, 150 rpm, 15 min temperature equilibration before adding glucose) was used for conducting fermentations, with the time-points (1, 3, 7, 9, 13 min) prepared as separate fermentations. Fermentations were stopped by centrifugation (4332 × g, 5 min, 4 ^{o}C) with 1.8 mL of the supernatant treated with 109.8 µL PCA (perchloric acid, 35 % (V/V)) to precipitate proteins. After 10 min of incubation on ice the samples were neutralized through the addition of 99 µL 7 M KOH, which was followed by another 10 min of incubation on ice, and finally removal of precipitated salts and proteins (20800 × g, 5 min, 4 ^{0}C). Samples were filtered (0.45 µm pvdf durapore membrane) before HPLC analysis.

An aminex-HPX 87H (Biorad, 300 × 7.8 mm) ion-exchange column was used to analyze the samples. The column temperature was 55 ^{o}C, with isocratic elution (0.005 M H_2SO_4) at a flow rate of 0.5 mL/min. The sample injection volumes were 5 µL and 20 µL (duplicate runs), with the detection unit consisting of a refractory index detector and an ultraviolet detector (210 nm).

5.2.2.2) Resolving NTP and NDP with ^{31}P NMR spectroscopy

This protocol is based on previous work (13). Fermentations were conducted in a similar manner as the HPLC fermentation product analysis; except that the extraction time-points were 5, 6, 7 and 8 min, or 3.5, 4.5, 5.5 and 6.5 min. Each time-point was again prepared as a separate fermentation.

Fermentations were stopped through the addition of 600 µL cold perchloric acid (21 % (w/V)), rigorous shaking, and three rounds of freezing (liquid nitrogen, 10 min) and thawing (30 ^{o}C water bath, 10 min). After placing samples on ice for 10 min, cellular fragments and proteins were removed by centrifugation (30 min, 0^{o}C, 4332 × g), with 3.4 mL of the supernatant removed and neutralized through the addition of 400 µL 2 M K_2CO_3. The salt precipitate was removed by centrifugation (0^{o}C, 4332 × g, 10 min), and after diluting the supernatant (3.2 mL) with 4 mL de-ionized water, the pH of samples was adjusted to 8.1 through the addition of 40 mM K_2CO_3. The samples were then

carefully decanted into small glass containers, and sealed with paper towels and rubber bands, before being lyophilized for approximately 24 h. The lyophilized samples were re-suspended in 700 µL of 36 mM EDTA (pH 8.2), and again centrifuged (20800 × g, 0°C, 10 min) to remove a white sediment. Five hundred µl were then placed in a 5 mm NMR tube, with the sample filled to 600 µL with a solution containing the internal standard TEP (250 µM final concentration) in the NMR solvent D_2O.

The samples were analyzed with a 300 MHz Varian NMR spectrometer, with the following parameters: pulse duration (5 µs), flip angle (45°), acquisition time (1.6 s), broadband ^1H decoupling (continuous), pre-acquisition time (1 s), transients (3840), spectral width (14705.88 Hz), frequency (121.34 MHz), sample spin (20 Hz), temperature (25 °C). Peaks were analyzed by integration (line-broadening 0.5 Hz). Cytoplasmic concentrations were determined by using the conversion factor 2.4 µl cytoplasmic volume/mg dry weight; total cellular volume was assumed as 3 µl/mg dry weight (36).

5.3) Enzyme activity determination

5.3.1) Optimization of a sonication procedure for preparation of cell free extracts

The wild type *Z. mobilis* (CP4) was used for the optimization of a sonication procedure for the preparation of cell free extracts. After harvesting (4332 × g, 15 min, 4 °C, OD 4) and re-suspension in buffer (20 mM MES-KOH (pH 6.5), 50 mM NaCl, 10 mM β-mercapthoethanol, 2 mM $MgCl_2$) at OD_{550} = 2.5 (final volume 8 mL), the culture was sonicated (intensity level 5). To dissipate the heat generated during sonication the culture was placed on ice and sonication was conducted in an intermittent fashion (15 s sonication cycles with 15 s breaks for the first 2 min, and 45 s breaks afterwards). Samples (500 µL) for glucose-6-phosphate dehydrogenase assays (used as an indicator of enzyme activity) were taken after every second sonication cycle. Each sample was centrifuged (3823 × g, 15 min, 4 °C), and glucose-6-phosphate dehydrogenase activity (NADH production rate) was determined over 30 s at room temperature (absorbance at

340 nm). The assay volume was 1 mL and contained the following components: 900 µL assay buffer (30 mM TRIS (pH 8 - HCl), 30 mM KCl, 1.11 mM NAD^+, 1.11 mM glucose 6-phosphate, 2.22 mM MgSO4); 100 µL cell extract.

5.3.2) Glucose-6-phosphate dehydrogenase, phosphoglycerate kinase and pyruvate kinase activity determination

A thermostatted spectrophotometer at 30 ^oC was used for the enzyme activity determination. Glucose-6-phosphate dehydrogenase activity was determined as discussed in the previous section. The phosphoglycerate kinase assay mixture containing the following components per 1 mL: 900 µL assay buffer (50 mM MES (pH 6.5), 30 mM KCl, 3 mM $MgCl_2$, 1 mL/L β-mercapthoethanol, 0.17 mM NADH, 1.11 mM ATP, 5.55 mM 3-phosphoglycerate, 11.11 U glyceraldehyde-3-phosphate dehydrogenase (EC 1.2.1.12)); 100 µL cell extract. The pyruvate kinase assay mixture contained the following components per 1 mL: 900 µL assay buffer (50 mM MES (pH 6.5), 30 mM KCl, 3 mM $MgCl_2$, 0.17 mM NADH, 0.55 mM ADP, 0.55 mM PEP, 11.11 U lactate dehydrogenase); 100 µL cell extract. An extinction coefficient of 6.3 $dm^3mmol^{-1}cm^{-1}$ for NADH was used for enzyme activity calculations.

5.3.3) Protein determination

The Lowry method was used to determine total protein (50). Standards of 0.005 % (w/V), 0.01 % (w/V), 0.02 % (w/V), 0.04 % (w/V), and 0.08 % (w/V) BSA were dissolved in distilled water. Three ml of a solution prepared in the following manner was added to the standards and suitably diluted cell extract (and left at room temperature in the dark for 10 min): solution A – 4 g NaOH, 20 g Na_2CO_3, 0.2 g K-Na-Tartrate in 1 L distilled water; solution B – 0.5 g $CuSO_4.5H_20$ in 100 mL distilled water; solution C – 12.25 mL solution A and 0.25 mL solution B mixed just before use. After incubation, 0.3 mL 50 % (V/V) Folin reagent (diluted with distilled water) was added to each sample and left at room temperature in the dark for a further 20 min. When incubation was complete the absorbance was measured spectrophotometrically at 750 nm.

5.4) Dry weight determination

A cellulose acetate filter (0.22 µm pore size, Osmonics) was dried for 4 min (330 W microwave), and cooled for 15 min in a dessicator containing silica gel before weighing. Cells were vacuum filtered with continual rinsing with de-ionized water. The filter with the cells was micro-waved for 8 min (330 W), and cooled afterwards in a dessicator for 15 min before weighing.

5.5) Reagents

MES buffer was purchased from AEC Amersham (Cleveland USA). ^{13}C-labelled glucose was purchased from Cambridge Isotope Laboratories (UK). The metabolite intermediates, enzymes, glucose, TEP, BSA and Folin reagent were purchased from Sigma (Steinheim, Germany). The other reagents were purchased from Merck (Darmstadt, Germany).

Bibliography

1) Swings, J. & De Ley, J. (1977) The biology of *Zymomonas*, *Bacteriological Reviews*. 41, 1 – 46.

2) Algar, E.M. & Scopes, R. (1985) Studies on cell – free metabolism: Ethanol production by extracts of *Zymomonas mobilis*, *Journal of Biotechnology*.2, 275 – 287.

3) Snoep, J.L., Arfman, N., Yomano, L.P., Westerhoff, H.V., Conway, T., O'Neal Ingram, L. (1996) Control of glycolytic flux in *Zymomonas mobilis* by glucose 6 – phosphate dehydrogenase activity, *Biotechnology and Bioengineering.* 51, 190 – 197.

4) Conway, T. (1992) The Entner – Doudoroff pathway: history, physiology and molecular biology, *FEMS Microbiology reviews.* 103, 1 – 28.

5) Fell, D. (1997) *Understanding the control of metabolism*, Portland Press Ltd. London.

6) Newsholme, E.A. & Start, C. (1973) *Regulation in metabolism*, John Wiley and Sons. London, New York, Sydney, Toronto.

7) Kacser, H & Burns, J.A. (1973) The control of flux, *Symposia of the Society for Experimental Biology.* 27, 65 – 104.

8) Heinrich, R & Rapoport, T. (1974) A linear steady – state treatment of enzymatic chains. General properties, control and effector strength, *European Journal of Biochemistry.* 42, 89 – 95.

9) Hofmeyr, J. – H. S. & Cornish – Bowden, A. (2000) Regulating the cellular economy of supply and demand, *FEBS Letters*. 476, 47 – 51.

10) Sprenger, G.A. (1996) Carbohydrate metabolism in *Zymomonas mobilis*: a catabolic highway with some scenic routes, *FEMS Microbiology letters.* 145, 301 - 307.

11) Dawes, E.A. & Large, P.J. (1970) Effect of starvation on the viability and cellular constituents of *Zymomonas anaerobia* and *Zymomonas mobilis, Journal of General Microbiology*. 60, 31 – 42.

12) de Graaf, R.A. (1998) *In vivo NMR spectroscopy. Principles and techniques*, Chichester: Wiley.

13) Barrow, K.D., Collins, J.G., Norton, R.S., Rogers, P.L., Smith, G.M. (1984) ^{31}P Nuclear Magnetic Resonance studies of the fermentation of glucose to ethanol by *Zymomonas mobilis, The journal of biological chemistry.* 259, 5711-5716.

14) De Graaf, A.A., Striegel, K., Wittig, R.M., Laufer, B., Schmitz, G., Wiechert, W., Sprenger, G.A., Sahm, H. (1999) Metabolic state of *Zymomonas mobilis* in glucose-, fructose-, and xylose-fed continuous cultures as analysed by ^{13}C- and ^{31}P-NMR spectroscopy, *Archives of Microbiology.* 171, 371-385.

15) Weisser, P., Krämer, R., Sahm, H., Sprenger, G.A. (1995) Functional expression of the glucose transporter of *Zymomonas mobilis* leads to restoration of glucose and fructose uptake in *Eschericia coli* mutants and provides evidence for its facilitator action, *Journal of Bacteriology.* 177, 3351 – 3354.

16) Parker, C., Barnell, W.O., Snoep, J.L., Ingram, L.O., Conway, T. (1995) Characterization of the *Zymomonas mobilis* glucose facilitator gene product (glf) in recombinant *Eschericia coli*: examination of transport mechanism, kinetics and the role of glucokinase in glucose transport, *Molecular Microbiology.* 15, 795 – 802.

17) Kirk, L.A. & Doelle, H.W. (1993) Rapid ethanol production from sucrose without byproduct formation, *Biotechnology Letters.* 15, 985 – 990.

18) Wiegert, T., Sahm, H., Sprenger, G.A. (1996) Export of the periplasmic NADP-containing glucose-fructose oxidoreductase of *Zymomonas mobilis*, *Archives of Microbiology.* 166, 32 – 41.

19) Loos, H., Krämer, R., Sahm, H., Sprenger, G.A. (1994) Sorbitol promotes growth of *Zymomonas mobilis* in high sugar-content environments: evidence for a physiological function of glucose-fructose oxidoreductase in osmoprotection, *Journal of Bacteriology.* 176, 7688 – 7693.

20) Zachariou, M. & Scopes, R.K. (1986) Glucose-fructose oxidoreductase, a new enzyme isolated from *Zymomonas mobilis* that is responsible for sorbitol production, *Journal of Bacteriology.*. 167, 863 – 869.

21) Preziosi, L., Michel, G.P.F., Baratti, J. (1990) Sucrose metabolism in *Zymomonas mobilis*, *Canadian Journal of Microbiology.* 36, 159 – 163.

22) Romano, A.H. & Conway, T. (1996) Evolution of carbohydrate metabolic pathways, *Research in Microbiology.* 147, 448 – 455.

23) Kalnenieks, U. (2006) Physiology of *Zymomonas mobilis*: Some unanswered questions, *Advances in Microbial Physiology.* 51, 73 – 117.

24) Dien, B.S., Cotta, M.A., Jeffries, T.W. (2003) Bacteria engineered for fuel ethanol Production: current status, *Applied Microbiology and Biotechnology.* 63, 258 – 266.

25) Lazdunski, A. & Belaich, J.P. (1972) Uncoupling in bacterial growth: ATP pool variation in *Zymomonas mobilis* cells in relation to different uncoupling conditions of growth, *Journal of General Microbiology.* 70, 187 – 197.

26) Reyes, L. & Scopes, R.K. (1991) Membrane – associated ATPase from *Zymomonas Mobilis*; purification and characterization, *Biochimica et Biophysica Acta.* 1068, 174 – 178.

27) Zikmanis, P., Kruce, R., Auzina, L. (1999) Molar growth yields of *Zymomonas Mobilis* on glucose after the transition from anaerobic to aerobic continuous growth, *Acta Biotechnologica.* 19, 69 – 75.

28) Belaich, J.P. & Senez, J.C. (1965) Influence of aeration and pantothenate on growth yields of *Zymomonas mobilis*, *Journal of Bacteriology.* 89, 1195 – 1200.

29) Kalnenieks, U., de Graaf, A.A., Bringer-Meyer, S., Sahm, H. (1993) Oxidative phosphorylation in *Zymomonas mobilis*, *Archives of Microbiology.* 160, 74 – 79.

30) Brown, G.C., Hafner, R.P., Brand, M.D. (1990) A 'top-down' approach to the determination of control coefficients in metabolic control theory, *European Journal of Biochemistry.* 188, 321 – 325.

31) Koebmann, B.J., Westerhoff, H.V., Snoep, J.L., Nilsson, D., Jensen, P.R. (2002) The glycolytic flux in *Eschericia coli* is controlled by the demand for ATP, *Journal of Bacteriology.* 184, 3909-3916.

32) Rohwer, J.M. & Hofmeyr, J-H.S. (2008) Identifying and characterizing regulatory metabolites with generalized supply-demand analysis, *Journal of Theoretical Biology.* 252, 546-554.

33) Shulman, R.G. & Rothman, D.L. (2005) *Metabolomics by In Vivo NMR*, John Wiley & Sons, Ltd.

34) James, T.L. (1999) Fundamentals of NMR, in *Nuclear Magnetic Resonance (NMR), Online Biophysics Textbook, Biophysical Society* (Gorenstein, D., ed.).

35) Barrow, K.D., Rogers P.L., Smith G.M. (1986) NMR studies of [1-^{2}H] glucose metabolism in *Zymomonas mobilis*, *European Journal of Biochemistry*. 157, 195-202.

36) Schoberth, S.M., Chapman, B.E., Kuchel, P.W., Wittig, R.M., Grotendorst, J., Jansen, P., DE Graaf, A.A. (1996) Ethanol transport in *Zymomonas mobilis* measured by using *in vivo* nuclear magnetic resonance spin transfer, *Journal of Bacteriology.* 178, 1756-1761.

37) Kacser, H. & Burns, J.A. (1979) Molecular democracy: who shares the controls?, *Biochem. Biochemical Society Transactions.* 7, 1149-1160.

38) Hofmeyr, J-H. S. & Rohwer, J.M. (1998) Control analysis of adenylate-conserving cycles in the absence or presence of adenylate kinase, in *BioThermoKinetics in the Post Genomic Era* (Larsson, C., Påhlman, I., Gustafsson, L., eds.) pp. 7-10, Chalmers Reproservice, Göteborg.

39) Snoep, J.L., Yomano, L.P., Westerhoff, H.V., Ingram, L.O (1995) Protein burden in *Zymomonas mobilis*: negative flux and growth control due to overproduction of glycolytic enzymes, *Microbiology.* 141, 2329-2337.

40) Arfman, N.A., Worrell, V., Ingram, L.O. (1992) Use of the *tac* promoter and *lacIq* for the controlled expression of *Zymomonas mobilis* fermentative genes in *Escherichia coli* and *Zymomonas mobilis, Journal of Bacteriology.* 174, 7370-7378.

41) Yomano, L.P., Scopes, R.K., Ingram, L.O. (1993) Cloning, sequencing, and expression of the *Zymomonas mobilis* phosphoglycerate mutase (*pgm*) in *Escherichia coli*, *Journal of Bacteriology*. 175, 3926-3933.

42) Lawford, H.G. & Rousseau, J.D. (1994) The pH-dependent energetic uncoupling of *Zymomonas* by acetic acid, *Humana Press Inc.* 45-46, 437-448.

43) Sáez-Miranda, J.C., Saliceti-Piazza, L., McMillan, J.D. (2006) Measurement and analysis of intracellular ATP levels in metabolically engineered *Zymomonas mobilis* fermenting glucose and xylose mixtures, *Biotechnology Progress.* 22, 359-368.

44) Kroukamp, O., Rohwer, J.M., Hofmeyr, J-H.S., Snoep, J.L. (2002) Experimental supply-demand analysis of anaerobic *yeast* energy metabolism, *Molecular Biology Reports.* 29, 203-209.

45) Doelle, H.W. (1981) Kinetic characteristics and regulatory mechanisms of glucokinase and fructokinase from *Zymomonas mobilis, Applied Microbiology and Biotechnology.* 14, 241-246.

46) Kim, I.S., Barrow, K.D., Rogers, P.L. (2000) Nuclear magnetic resonance studies of acetic acid inhibition of Rec *Zymomonas mobilis* ZM4(pZB5), *Applied Biochemistry and Biotechnology*. 84-86, 357-370.

47) Bergmeyer, H.-U. (1963) *Methods of enzymatic analysis*, Academic Press New York London.

48) Altintas, M.M., Eddy, C.K., Zhang, M., McMillan, J.D., Kompala, D.S. (2006) Kinetic modeling to optimize pentose fermentation in *Zymomonas mobilis*, *Biotechnology and Bioengineering*. 94, 273-295.

49) Du Preez, F.B., Conradie, R., Penkler, G.P., Holm, F., Van Dooren, F.L.J., Snoep, J.L. (2008) A comparative analysis of kinetic models of erythrocyte glycolysis, *Journal of Theoretical Biology.* 252, 488-496.

50) Lowry, O.H., Rosbrough, N.J., Farr, A.L., Randall, R.J. (1951) Protein measurement with the Folin phenol reagent, *Journal of Biological Chemistry.* 193, 265-275.